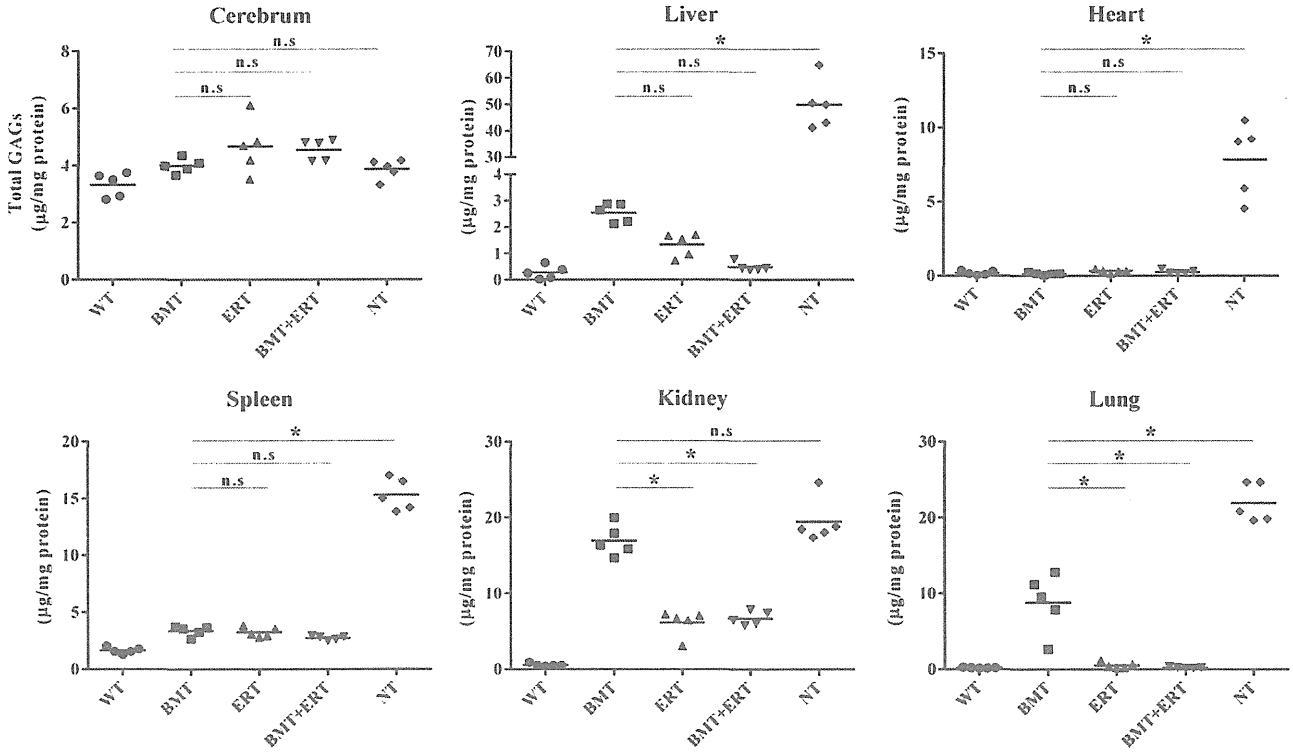

Fig. 4. Corrections of total GAGs accumulation in various tissues. The tGAGs in cerebrum, liver, heart, spleen, kidney and lung was assayed using Alcian blue method. Amount of tGAGs is expressed as μg/mg protein. Each symbol represents a data of individual mouse. Horizontal bar indicates mean value. Difference of tGAGs among 3 treatment groups and NT group was compared using one-way ANOVA. Asterisk indicates $P < 0.05$. "n.s" indicates no significant difference.

3.5. Impact of elevated IDS activity on pathologic GAGs levels

Since there was no additive effect of ERT to BMT at reducing tGAGs in the cerebrum, liver, heart and spleen, we had the opportunity to utilize a more sensitive and specific assay that detects only pathologic GAGs (pGAGs, a selective measure of GAG fragments generated in the lysosome due to the deficiency of IDS). In the cerebrum (Fig. 5), none of treatments reduced pGAGs levels. It is worth noting though that the difference in cerebrum pGAG levels between WT mice and NT MPS II mice was more obvious than tGAGs. In the liver (Fig. 5), pGAGs were significantly reduced by BMT, ERT and BMT + ERT treatments compared to untreated controls. However, the extent of reduction was not statistically difference among the three treatment groups. Like noted earlier with tGAGs, there was a suggestion that ERT conferred an additive effect to BMT; however the effect was not statistically different. In the heart (Fig. 5), all the treatments significantly reduced pGAGs. ERT reduced pGAGs more profoundly than BMT and ERT provided an additive effect to BMT.

In summary, none of the treatment reduced pGAGs in the cerebrum. In the liver, the results with pGAG were the same as noted with tGAG. In the heart, we demonstrated an additive effect of ERT to BMT but this could not be proven in tGAGs. These results also indicated that pGAGs are a better indicator than tGAGs of therapeutic effect of the treatments in the cerebrum and heart.

3.6. Impact of elevated IDS activity on total urinary GAG levels

All the treatments reduced urinary tGAGs to almost normal levels and no statistical difference among all treatment groups (Fig. 6). Thus,

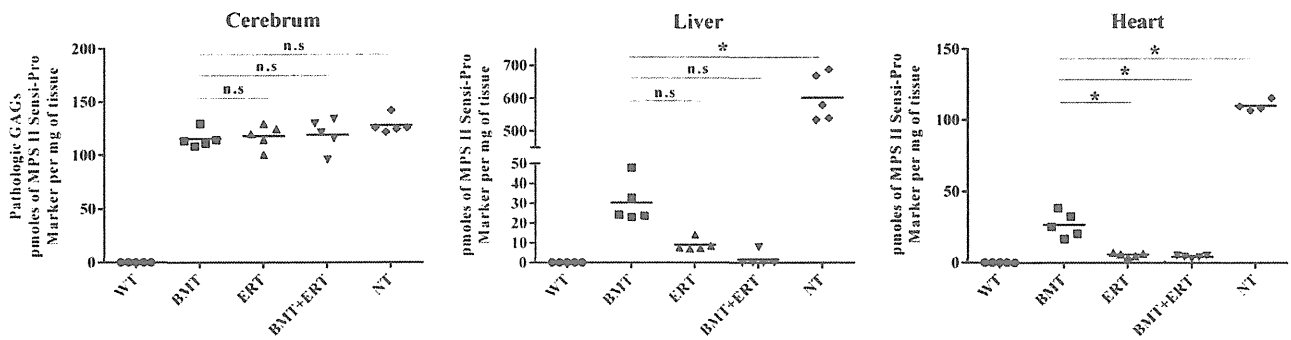

Fig. 5. Pathologic GAGs accumulation in tissues. pGAGs were measured in cerebrum, liver and heart as described in Methods. The amount of pGAGs is expressed as pmols of MPS II Sensi-Pro Marker per mg of tissue. Each symbol represents a data of individual mouse. Horizontal bar indicates mean value. Difference of pGAGs among 3 treatment groups and NT group was compared using one-way ANOVA. Asterisk indicates $P < 0.05$. "n.s" indicates no significant difference.

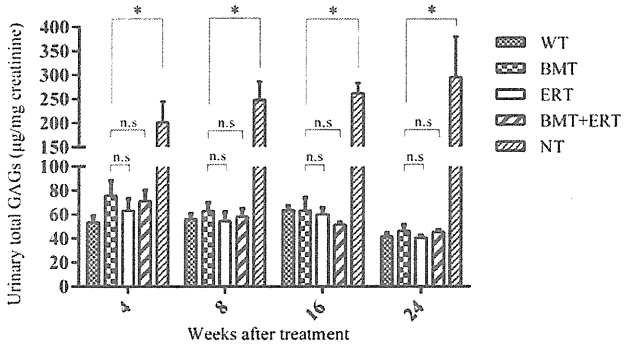

Fig. 6. Corrections of urinary total GAGs excretion. Urinary tGAGs were assayed using Alcian blue method. Amount of urinary tGAGs is expressed as μg/mg creatinine. The data of each group are shown as mean ± SEM (WT: n = 7, BMT: n = 5, ERT: n = 5, BMT + ERT: n = 5, NT: n = 6). Difference of tGAGs among 3 treatment groups and NT group was compared using one-way ANOVA. Asterisk indicates $P < 0.05$. "n.s" indicates no significant difference.

any additive effect of ERT to BMT or difference in efficacy between BMT and ERT could not be observed.

3.7. Growth of MPS II mice

Body weights of mice were also monitored in each treatment and control mice (Fig. 7). Similar to human MPS II patients [21], MPS II mice also exhibited greater weights. All treatments suppressed the overgrowth of MPS II mice when measured at 27 weeks post-treatment. However, ERT did not provide an additive effect to BMT and there was no statistically significant difference between mice treated by BMT and ERT.

3.8. IgG antibody against IDS in ERT groups

In some mice, anti IgG antibodies developed against the recombinant enzyme (Supplemental Fig. 2). However, these antibody titers were very low compared to titers developed following ERT in other lysosomal storage disease mouse models. For example, when we assayed the IgG antibody titer against infused enzyme in the mouse model of Pompe disease employing a similar method to this study we had to dilute serum 20,000 times or more to put in OD 450 nm values in the linear range of standard curve [22]. However, in this study, OD450 nm values were in linear range using 100 times diluted serum. When the serum was diluted more, the antibody titer was under the detection limit.

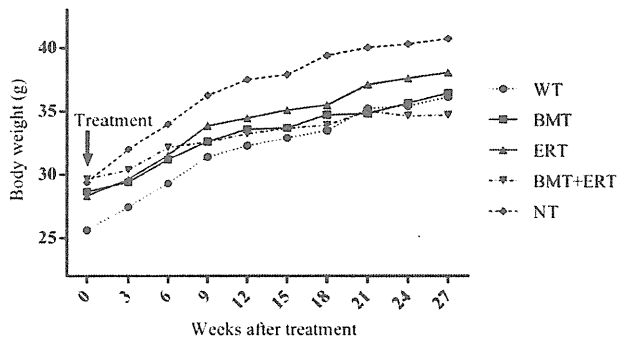

Fig. 7. Suppression of over growth by treatment. The body weight of mice was measured at every 3 weeks from 9 weeks of age until sacrifice. The body weight of mice from each group is shown as mean values. Difference of body weight at 27 weeks after treatment among 3 treatment groups and NT group was compared using one-way ANOVA. "n.s" indicates no significant difference. (ERT or BMT or BMT + ERT vs NT; $P < 0.05$, BMT vs BMT + ERT; n.s, ERT vs BMT; n.s).

4. Discussion

In early 1980s, first report described the effectiveness of BMT for MPS I [23]. Subsequently, BMT was performed in many MPS I patients with encouraging results [24]. BMT was particularly effective at addressing the CNS involvement of MPS I patients when BMT was performed in patients who were <2 years old and had an IQ ≥ 70. Animal studies also demonstrated a reduction of GAGs in brain following BMT [25]. In contrast to MPS I, there is huge controversy for indicating BMT for MPS II patients [10,11]. BMT is not indicated for MPS II because of the limited efficacy at correcting the CNS disease of MPS II patients [12–15]. However, a recent retrospective study of Japanese MPS II patients who received BMT demonstrated that this therapy was effective at addressing the CNS disease of mild type MPS II (MPS IIB) and their valvular disease [16]. However, as all the studies were in MPS II patients, pathological and biochemical data are not available to support these findings. To address this issue, we performed BMT on MPS II mice to clarify whether pathological, biochemical changes were evident. Our studies indicated no evidence of an increase in enzyme activity or reduction of GAGs in the brain of transplanted MPS II mice. Pathological analysis of brain sections was very hard to interpret because of the limited amounts of storage material in the brain of MPS II mice (data not shown). Moreover no neurofunctional improvement was observed by BMT (data not shown). From these observations, we conclude that BMT does not appear to be effective in treating the CNS disease in MPS II, similar to MPS III [26]. However, it is possible that the assays that we used here were not sufficiently sensitive to monitor therapeutic effects of the treatments to CNS involvement of MPS II. As an alternative approach to treat the CNS disease, other investigators are using genetically-modified donor bone marrow cells to enhance the expression and secretion of the lysosomal enzyme prior to transplantation. The effectiveness of this approach to treat the CNS disease has now been reported in MPS III mice [27]. We did observe a reduction in GAGs in many visceral diseases by BMT, as expected.

ERT for MPS II was approved in 2006 in US and EU, and in 2007 in Japan. ERT improved the performance of MPS II patients on the 6 minute walk test and their predicted FVC [3–5]. Although it is clear that ERT offers a therapeutic effect, the cost of this therapy is very high and requires lifelong repeated administration [9]. BMT has the possibility to overcome these problems. However, it is not known which is more effective, BMT or ERT. From our study, ERT was more effective than BMT at reducing GAGs in heart, kidney and lung. In studies of ERT for LSDs other than MPS II, many reports suggested that antibodies against the infused enzyme can inhibit the therapeutic efficacy of ERT, and have been particularly well described in Pompe disease [28,29]. In our mice studies, antibody titers against the administered enzyme were low; thus we might have overestimated the efficacy of ERT. From our experience, if the immunological response against the infused enzyme is controlled, ERT is superior to BMT, at least in a few organs.

Before the availability of ERT, BMT was carried out in a small number of MPS II patients. One report indicated that a single dose of ERT to already transplanted MPS VI patient caused further reduction of urinary GAGs [30]. Another report indicated that supplementing BMT treated MPS VI patients with ERT caused further improvement of several clinical parameters, including joint movement, outcome of the 12 minute walk test and the outcome of the 3 minute stair-climbing test [31]. Several studies reported that ERT in the peritransplanted period reduced the BMT-related morbidity and mortality in children with MPS I and VI. However, these studies addressed to safety issue of BMT not to additive therapeutic effect of ERT to BMT [32–36]. Moreover, MPS I and VI are different diseases from MPS II. Thus, the results of MPS I and VI might not relevant to MPS II. In this study, we introduced ERT to already transplanted MPS II mice and found an additive effect of ERT to BMT in the heart, kidney and lung, at least in terms of reducing GAG levels. Taken together, an additive effect of ERT to BMT was observed in tissues which ERT had a superior effect to BMT. From these observations, it

might be worthwhile to perform ERT to already transplanted MPS II patients, especially as the effects of BMT are limited. However, it is still not known if more profound reduction of GAGs causes a more robust improvement in clinical signs of MPS II. Hence, indicating ERT as a supplement to BMT should be carefully determined.

Finally, we assayed tissue pGAGs and tGAGs to monitor the therapeutic effects of treatments in MPS II mice. From our observations, there was very little difference between tGAGs in brain from WT and MPS II mice (Fig. 4); however, there was a significant difference between pGAGs in brain from WT and MPS II mice (Fig. 5). Thus, like MPS I [37], pGAGs are a better biomarker than tGAGs to monitor the therapeutic effect in MPS II specifically. These new pGAG quantitation methods provide a simple, rapid diagnostic strategy for MPS I, II, IIIA, IIIB, IIIC, IIID, VI and VII using samples of urine, blood and dried blood spots. Analysis of the non-reducing end glycans provides a method for monitoring not only enzyme replacement but also substrate reduction therapies and serves as a discovery tool for uncovering novel biomarkers and new forms of mucopolysaccharidoses [38]. In conclusion, BMT and ERT alone or even as a combination, have a limited positive effect on the brain disease of MPS II mice. ERT seems to be superior to BMT at reducing GAGs in tissues provided that the immunological responses against the infused enzyme are low. ERT conferred an additive effect to BMT at reducing GAGs in several visceral organs. Finally, pGAGs are a better biomarker to monitor the therapeutic effect of MPS II.

Supplementary data to this article can be found online at http://dx.doi.org/10.1016/j.ymgme.2013.09.013.

Conflict of interest

T. Ohashi, H. Ida and Y. Eto have active research support from Genzyme Japan Co., Ltd. and Shire Japan Co., Ltd. These activities have been fully disclosed and are managed under a Memorandum of Understanding with the Conflict of Interest Resolution Board of The Jikei University School of Medicine.

Acknowledgments

Authors wish to thank Joseph Muenzer at University of North Carolina at Chapel Hill for providing us the MPS II mice, Hideto Morimoto at JCR Pharmaceuticals Company Limited for providing us antibody against human IDS and Genzyme Japan Co., Ltd. for providing us Idursulfase. We also thank Seng Cheng at Genzyme Corporation for critically reviewing our manuscript, Taku Sato at Tokyo Medical and Dental University for helping us flow cytometry study and Sayoko Iizuka and Eiko Kaneshiro at The Jikei University School of Medicine for their excellent technical assistance. Finally we thank members of Laboratory Animal Facility at The Jikei University School of Medicine for helping us with the animal studies. This work was supported by grant of the Vehicle Racing Commemorative Foundation.

References

[1] G. Bach, F. Eisenberg Jr., M. Cantz, E.F. Neufeld, The defect in the Hunter syndrome: deficiency of sulfoiduronate sulfatase, Proc. Natl. Acad. Sci. U. S. A. 70 (1973) 2134–2138.
[2] R. Martin, M. Beck, C. Eng, R. Giugliani, P. Harmatz, V. Munoz, J. Muenzer, Recognition and diagnosis of mucopolysaccharidosis II (Hunter syndrome), Pediatrics 121 (2008) e377–e386.
[3] J. Muenzer, J.E. Wraith, M. Beck, R. Giugliani, P. Harmatz, C.M. Eng, A. Vellodi, R. Martin, U. Ramaswami, M. Gucsavas-Calikoglu, S. Vijayaraghavan, S. Wendt, A.C. Puga, B. Ulbrich, M. Shinawi, M. Cleary, D. Piper, A.M. Conway, A. Kimura, A phase II/III clinical study of enzyme replacement therapy with idursulfase in mucopolysaccharidosis II (Hunter syndrome), Genet. Med. 8 (2006) 465–473.
[4] T. Okuyama, A. Tanaka, Y. Suzuki, H. Ida, T. Tanaka, G.F. Cox, Y. Eto, T. Orii, Japan Elaprase Treatment (JET) study: idursulfase enzyme replacement therapy in adult patients with attenuated Hunter syndrome (Mucopolysaccharidosis II, MPS II), Mol. Genet. Metab. 99 (2010) 18–25.
[5] J. Muenzer, M. Beck, C.M. Eng, R. Giugliani, P. Harmatz, R. Martin, U. Ramaswami, A. Vellodi, J.E. Wraith, M. Cleary, M. Gucsavas-Calikoglu, A.C. Puga, M. Shinawi, B. Ulbrich, S. Vijayaraghavan, S. Wendt, A.M. Conway, A. Rossi, D.A. Whiteman, A. Kimura, Long-term, open-labeled extension study of idursulfase in the treatment of Hunter syndrome, Genet. Med. 13 (2011) 95–101.
[6] J.E. Wraith, M. Scarpa, M. Beck, O.A. Bodamer, L. De Meirleir, N. Guffon, A. Meldgaard Lund, G. Malm, A.T. Van der Ploeg, J. Zeman, Mucopolysaccharidosis type II (Hunter syndrome): a clinical review and recommendations for treatment in the era of enzyme replacement therapy, Eur. J. Pediatr. 167 (2008) 267–277.
[7] S. Al Sawaf, E. Mayatepek, B. Hoffmann, Neurological findings in Hunter disease: pathology and possible therapeutic effects reviewed, J. Inherit. Metab. Dis. 31 (2008) 473–480.
[8] Y. Sato, M. Fujiwara, H. Kobayashi, H. Ida, Massive accumulation of glycosaminoglycans in the aortic valve of a patient with Hunter syndrome during enzyme replacement therapy, Pediatr. Cardiol. (2013)(in press).
[9] K. Wyatt, W. Henley, L. Anderson, R. Anderson, V. Nikolaou, K. Stein, L. Klinger, D. Hughes, S. Waldek, R. Lachmann, A. Mehta, A. Vellodi, S. Logan, The effectiveness and cost-effectiveness of enzyme and substrate replacement therapies: a longitudinal cohort study of people with lysosomal storage disorders, Health Technol. Assess. 16 (2012) 1–543.
[10] C. Peters, C.G. Steward, National Marrow Donor Program, International Bone Marrow Transplant Registry, Working Party on Inborn Errors, European Bone Marrow Transplant Group, Hematopoietic cell transplantation for inherited metabolic diseases: an overview of outcomes and practice guidelines, Bone Marrow Transplant. 31 (2003) 229–239.
[11] J.J. Boelens, Trends in haematopoietic cell transplantation for inborn errors of metabolism, J. Inherit. Metab. Dis. 29 (2006) 413–420.
[12] E.G. Shapiro, L.A. Lockman, M. Balthazor, W. Krivit, Neuropsychological outcomes of several storage diseases with and without bone marrow transplantation, J. Inherit. Metab. Dis. 18 (1995) 413–429.
[13] E.J. McKinnis, S. Sulzbacher, J.C. Rutledge, J. Sanders, C.R. Scott, Bone marrow transplantation in Hunter syndrome, J. Pediatr. 129 (1996) 145–148.
[14] A. Vellodi, E. Young, A. Cooper, V. Lidchi, B. Winchester, J.E. Wraith, Long-term follow-up following bone marrow transplantation for Hunter disease, J. Inherit. Metab. Dis. 22 (1999) 638–648.
[15] N. Guffon, Y. Bertrand, I. Forest, A. Fouilhoux, R. Froissart, Bone marrow transplantation in children with Hunter syndrome: outcome after 7 to 17 years, J. Pediatr. 154 (2009) 733–737.
[16] A. Tanaka, T. Okuyama, Y. Suzuki, N. Sakai, H. Takakura, T. Sawada, T. Tanaka, T. Otomo, T. Ohashi, M. Ishige-Wada, H. Yabe, T. Ohura, N. Suzuki, K. Kato, S. Adachi, R. Kobayashi, H. Mugishima, S. Kato, Long-term efficacy of hematopoietic stem cell transplantation on brain involvement in patients with mucopolysaccharidosis type II: a nationwide survey in Japan, Mol. Genet. Metab. 107 (2012) 513–520.
[17] A.R. Garcia, J. Pan, J.C. Lamsa, J. Muenzer, The characterization of a murine model of mucopolysaccharidosis II (Hunter syndrome), J. Inherit. Metab. Dis. 30 (2007) 924–934.
[18] T. Yokoi, H. Kobayashi, Y. Shimada, Y. Eto, N. Ishige, T. Kitagawa, M. Otsu, H. Nakauchi, H. Ida, T. Ohashi, Minimum requirement of donor cells to reduce the glycolipid storage following bone marrow transplantation in a murine model of Fabry disease, J. Gene Med. 13 (2011) 262–268.
[19] T. Higuchi, H. Shimizu, T. Fukuda, S. Kawagoe, J. Matsumoto, Y. Shimada, H. Kobayashi, H. Ida, T. Ohashi, H. Morimoto, T. Hirato, K. Nishino, Y. Eto, Enzyme replacement therapy (ERT) procedure for mucopolysaccharidosis type II (MPS II) by intraventricular administration (IVA) in murine MPS II, Mol. Genet. Metab. 107 (2012) 122–128.
[20] R. Lawrence, J.R. Brown, K. Al-Mafraji, W.C. Lamanna, J.R. Beitel, G.J. Boons, J.D. Esko, B.E. Crawford, Disease-specific non-reducing end carbohydrate biomarkers for mucopolysaccharidoses, Nat. Chem. Biol. 8 (2012) 197–204.
[21] A. Rozdzynska, A. Tylki-Szymanska, A. Jurecka, J. Cieslik, Growth pattern and growth prediction of body height in children with mucopolysaccharidosis type II, Acta Paediatr. 100 (2011) 456–460.
[22] T. Ohashi, S. Iizuka, Y. Shimada, T. Higuchi, Y. Eto, H. Ida, H. Kobayashi, Administration of anti-CD3 antibodies modulates the immune response to an infusion of alpha-glucosidase in mice, Mol. Ther. 20 (2012) 1924–1931.
[23] J.R. Hobbs, K. Hugh-Jones, A.J. Barrett, N. Byrom, D. Chambers, K. Henry, D.C. James, C.F. Lucas, T.R. Rogers, P.F. Benson, L.R. Tansley, A.D. Patrick, J. Mossman, E.P. Young, Reversal of clinical features of Hurler's disease and biochemical improvement after treatment by bone-marrow transplantation, Lancet 2 (1981) 709–712.
[24] J. Muenzer, J.E. Wraith, L.A. Clarke, International Consensus Panel on Management and Treatment of Mucopolysaccharidosis, Mucopolysaccharidosis I: management and treatment guidelines, Pediatrics 123 (2009) 19–29.
[25] D.A. Wolf, A.W. Lenander, Z. Nan, E.A. Braunlin, K.M. Podetz-Pedersen, C.B. Whitley, P. Gupta, W.C. Low, R.S. McIvor, Increased longevity and metabolic correction following syngeneic BMT in a murine model of mucopolysaccharidosis type I, Bone Marrow Transplant. 47 (2012) 1235–1240.
[26] A.A. Lau, H. Hannouche, T. Rozaklis, S. Hassiotis, J.J. Hopwood, K.M. Hemsley, Allogeneic stem cell transplantation does not improve neurological deficits in mucopolysaccharidosis type IIIA mice, Exp. Neurol. 225 (2010) 445–454.
[27] A. Langford-Smith, F.L. Wilkinson, K.J. Langford-Smith, R.J. Holley, A. Sergijenko, S.J. Howe, W.R. Bennett, S.A. Jones, J. Wraith, C.L. Merry, R.F. Wynn, B.W. Bigger, Hematopoietic stem cell and gene therapy corrects primary neuropathology and behavior in mucopolysaccharidosis IIIA mice, Mol. Ther. 20 (2012) 1610–1621.
[28] P.S. Kishnani, P.C. Goldenberg, S.L. DeArmey, J. Heller, D. Benjamin, S. Young, D. Bali, S.A. Smith, J.S. Li, H. Mandel, D. Koeberl, A. Rosenberg, Y.T. Chen, Cross-reactive immunologic material status affects treatment outcomes in Pompe disease infants, Mol. Genet. Metab. 99 (2010) 26–33.
[29] S.G. Banugaria, S.N. Prater, Y.K. Ng, J.A. Kobori, R.S. Finkel, R.L. Ladda, Y.T. Chen, A.S. Rosenberg, P.S. Kishnani, The impact of antibodies on clinical outcomes in diseases treated with therapeutic protein: lessons learned from infantile Pompe disease, Genet. Med. 13 (2011) 729–736.

[30] C.B. Whitley, J.R. Utz, Maroteaux–Lamy syndrome (mucopolysaccharidosis type VI): a single dose of galsulfase further reduces urine glycosaminoglycans after hematopoietic stem cell transplantation, Mol. Genet. Metab. 101 (2010) 346–348.
[31] Y.B. Sohn, S.W. Park, S.H. Kim, S.Y. Cho, S.T. Ji, E.K. Kwon, S.J. Han, S.J. Oh, Y.J. Park, A.R. Ko, K.H. Paik, J. Lee, D.H. Lee, D.K. Jin, Enzyme replacement therapy improves joint motion and outcome of the 12-min walk test in a mucopolysaccharidosis type VI patient previously treated with bone marrow transplantation, Am. J. Med. Genet. A 58A (2012) 1158–1163.
[32] S.S. Grewal, R. Wynn, J.E. Abdenur, B.K. Burton, M. Gharib, C. Haase, R.J. Hayashi, S. Shenoy, D. Sillence, G.E. Tiller, M.E. Dudek, A. van Royen-Kerkhof, J.E. Wraith, P. Woodard, G.A. Young, N. Wulffraat, C.B. Whitley, C. Peters, Safety and efficacy of enzyme replacement therapy in combination with hematopoietic stem cell transplantation in Hurler syndrome, Genet. Med. 7 (2005) 143–146.
[33] J. Cox-Brinkman, J.J. Boelens, J.E. Wraith, A. O'meara, P. Veys, F.A. Wijburg, N. Wulffraat, R.F. Wynn, Haematopoietic cell transplantation (HCT) in combination with enzyme replacement therapy (ERT) in patients with Hurler syndrome, Bone Marrow Transplant. 38 (2006) 17–21.
[34] J. Tolar, S.S. Grewal, K.J. Bjoraker, C.B. Whitley, E.G. Shapiro, L. Charnas, P.J. Orchard, Combination of enzyme replacement and hematopoietic stem cell transplantation as therapy for Hurler syndrome, Bone Marrow Transplant. 41 (2008) 531–535.
[35] R.F. Wynn, J. Mercer, J. Page, T.F. Carr, S. Jones, J.E. Wraith, Use of enzyme replacement therapy (Laronidase) before hematopoietic stem cell transplantation for mucopolysaccharidosis I: experience in 18 patients, J. Pediatr. 154 (2009) 135–139.
[36] D. Sillence, K. Waters, S. Donaldson, P.J. Shaw, C. Ellaway, Combined enzyme replacement therapy and hematopoietic stem cell transplantation in mucopolysaccharidosis type VI, JIMD Rep. 2 (2012) 103–106.
[37] P.I. Dickson, N.M. Ellinwood, J.R. Brown, R.G. Witt, S.Q. Le, M.B. Passage, M.U. Vera, B.E. Crawford, Specific antibody titer alters the effectiveness of intrathecal enzyme replacement therapy in canine mucopolysaccharidosis I, Mol. Genet. Metab. 106 (2012) 68–72.
[38] R. Lawrence, J.R. Brown, F. Lorey, P.I. Dickson, B.E. Crawford, J.D. Esko, Glycan-based biomarkers for mucopolysaccharidoses, Mol. Genet. Metab. 111 (2013) 73–83.

Molecular Genetics and Metabolism xxx (2013) xxx–xxx

Contents lists available at ScienceDirect

Molecular Genetics and Metabolism

journal homepage: www.elsevier.com/locate/ymgme

A practical fluorometric assay method to measure lysosomal acid lipase activity in dried blood spots for the screening of cholesteryl ester storage disease and Wolman disease

Takenori Dairaku [a], Takeo Iwamoto [b], Minami Nishimura [a], Masahiro Endo [a], Toya Ohashi [c,d], Yoshikatu Eto [a,*]

[a] Advanced Clinical Research Center, Southern TOHOKU Research Institute for Neuroscience, Fukushima, Japan
[b] Division of Biochemistry, Core Research Facilities, The Jikei University School of Medicine, Tokyo, Japan
[c] Department of Pediatrics, The Jikei University School of Medicine, Tokyo, Japan
[d] Department of Gene Therapy, The Jikei University School of Medicine, Tokyo, Japan

ARTICLE INFO

Article history:
Received 24 September 2013
Received in revised form 10 November 2013
Accepted 10 November 2013
Available online xxxx

Keywords:
4-Methylumbelliferone
Excitation wavelength
Full width at half maximum
Lysosomal acid lipase
Cholesteryl ester storage disease
Wolman disease

ABSTRACT

Fluorometric measurements of 4-methylumbelliferone (4-MU) are generally used to screen lysosomal storage diseases (LSDs) using dried blood spots (DBSs). However, in DBS, it is difficult to measure lysosomal acid lipase (LAL) activity due to the influence of other lipases in whole blood. Recently, Hamilton used a fluorometric enzyme assay with 4-MU derivatives to measure the LAL activity in DBS. This method requires mercury chloride as stopping reagent, and the fluorescence intensity of 4-MU was measured at an acidic pH. We report a revised method to measure the LAL activity without using toxic mercury chloride and to measure the fluorescence intensity of 4-MU at a basic pH. For this measurement, we established a more practical method that does not require mercury chloride.

The LAL activity in DBS was measured in 51 normal controls, seven obligate carriers and seven patients with CESD. The average LAL activities ± SD in the DBS from the normal, obligate carriers and CESD patients were 0.68 ± 0.2 (range: 0.3–1.08), 0.21 ± 0.1 (range: 0.11–0.41) and 0.02 ± 0.02 (range: 0–0.06) nmol/punch/h, respectively. There was a significant difference between the normal and the CESD. Our method does not require toxic mercury chloride and is an appropriate revised enzyme assay using DBS for screening patients with CESD.

1. Introduction

Cholesteryl ester storage disease (CESD) and Wolman disease (WD) are recessive autosomal disorders caused by a lysosomal acid lipase (LAL; EC 3.1.1.13) deficiency that hydrolyzes cholesteryl esters and triglycerides [1,2]. Clinically, WD is an infantile form of LAL deficiency characterized by marked hepatosplenomegaly, adrenal calcification and a failure to thrive, while CESD is a late onset form with hepatomegaly, microvesicular steatosis and cirrhosis.

Furthermore, enzyme replacement therapy for patients with LAL deficiency has recently been developed using recombinant enzymes produced by egg whites from transgenic *Gallus* [3]. Therefore, early diagnosis and treatment for WD and CESD require a simple diagnosis method using dried blood spots (DBSs). In particular, WD usually takes a rapid clinical course and requires early treatment via enzyme replacement therapy after screening newborns. Therefore, it is essentially necessary to establish an accurate and appropriate procedure to measure the LAL activity using DBS.

A fluorometric assay using 4-methylumbelliferone (4-MU) derivatives for measuring the LAL activity in fibroblasts was first reported by Guy in 1978 [4]. In this method, 4-methylumbelliferyl-palmitate (4-MUP) was used as an enzyme substrate, and the hydrolysis of this substrate occurred at acidic pH. The fluorescence intensity of the released 4-MU was measured at ~pH 9.5. However, in whole blood, it was difficult to measure the LAL activity due to the influence of other lipases in whole blood. Consequently, DBSs were not used to measure the LAL activity.

Currently, DBS samples are widely used to screen newborns for inborn metabolic errors [5], and fluorometric enzyme assay methods using 4-MU derivatives are commonly used to screen DBS for several lysosomal storage disorders (LSDs) [6]. Hamilton discovered a fluorometric measurement system using 4-MU derivatives to assess the LAL activity in DBS in 2012 [7]. In this method, 4-MUP was used as a substrate, and the enzymatic reaction was performed in the presence and absence of a LAL-specific inhibitor (Lalistat2). The released 4-MU was measured at an "acidic pH (~pH 4)" with mercury chloride.

In diagnostic LSD methods using DBS, the fluorescence intensity of 4-MU has been measured at "basic pHs (greater than pH 10)" [6].

Abbreviations: 4-MU, 4-methylumbelliferone; LAL, lysosomal acid lipase; DBS, dried blood spots; LSD, lysosomal storage disorders; CESD, cholesteryl ester storage disease; WD, Wolman disease; 4-MUP, 4-methylumbelliferyl-palmitate; FWHM, full width at half maximum.

* Corresponding author at: Advanced Clinical Research Center, Southern TOHOKU Research Institute for Neuroscience, 7-115, Yatuyamada, Koriyama, Fukushima 963-8563, Japan.
E-mail address: yosh@sepia.ocn.ne.jp (Y. Eto).

1096-7192/$ - see front matter © 2013 Elsevier Inc. All rights reserved.
http://dx.doi.org/10.1016/j.ymgme.2013.11.003

To date, a LAL enzyme assay method used to measure the released 4-MU under basic conditions has not been reported. At "basic pH", the optimal excitation wavelength required to measure the amount of released 4-MU is usually 365 nm. However, at "acidic pHs (~pH 4)", 355 nm was used for the excitation wavelength [7], and this method could differentiate between normal, carrier and CESD patients. The pH was significantly different between the former and latter cases, but the excitation wavelength was nearly the same, although the excitation wavelength of 4-MU is pH-dependent [8,9].

Regarding the optical filter, the full width at half maximum (FWHM) provides important information that can be used to measure the activity of the released 4-MU correctly. Because the optical filter with a wide FWHM value, it can concentrate light from a larger wavelength and detect additional fluorescence signals. However, because distinguishing between similar fluorescence wavelengths is difficult with these optical filters, it cannot be used normally when the fluorescence spectrum overlaps. These critical points used to measure a more precise wavelength for 4-MU have not been demonstrated in previous studies [6,7]. In the present study, we measured the excitation and mission spectra of 4-MU at several different pH values to observe the relationship between the pH and wavelength and to determine a suitable optical filter for measuring the LAL activity.

Based on these fundamental parameters, we have established a better enzyme assay method for measuring the LAL activity by modifying Hamilton's method [7].

2. Materials and methods

2.1. DBS samples

The 51 normal (adults) DBS samples (EDTA-blood) were obtained with informed consent by Dr. Yoshikatu Eto. The seven CESD and the seven obligate carrier DBS samples (EDTA-blood) were provided by Synageva BioPharma (Lexington, Massachusetts, USA) and Dr. John Hamilton (Department of Biochemistry, Yorkhill Hospital, UK). The samples were stored at 4 °C until analysis. This study was approved by the Ethics Committee of the Southern TOHOKU Research Institute for Neuroscience.

2.2. Reagents and equipment

4-Piperidinyl-1,2,5-thiadiazolyl-3-morpholine carboxylate (Lalistat2) was provided by Chemical Tools. 4-Methylumbelliferyl palmitate(4-MUP) was obtained from Santa Cruz Biotechnology. 4-Methylumbelliferone (4-MU), dimethyl sulfoxide (DMSO) and the cardiolipin solution were purchased from Sigma-Aldrich. Sodium acetate and acetic acid were obtained from Wako Pure Chemical Industries. The filter paper and black 96-well assay plates were purchased from Toyo Roshi Kaisha, Ltd., and Nunc, respectively. The fluorescence intensity was measured with a Corona MTP810 fluorescence microplate reader. A 365-nm filter (full width at half maximum (FWHM): 6 nm) was used for excitation, and a 450-nm filter (FWHM: 12 nm) was used for emission. The excitation and emission spectra were measured with a Shimadzu RF-5300PC spectrofluorometer.

2.3. Excitation and emission spectra

The excitation and emission spectra of 20 nM aqueous 4-MU were measured using a Shimadzu RF-5300PC spectrofluorometer at pH values 4.1, 7.1, 8.4 and 10.1. The excitation spectra were collected at 450 nm, and the emission spectra were collected at 320 nm or 365 nm. A pH titration was performed by adding 0.025–1.0 M NaOH or 0.025–1.0 M HCl to 20 nM aqueous 4-MU (1 nmol/50 mL). A 3-mL aliquot of the 4-MU solution was removed from the beaker at each titration point, and the fluorescence intensity of the sample was measured in a disposable plastic cuvette. The excitation and emission spectra were recorded, and the solution was returned to the beaker. The final volume of the 4-MU solution was 52.6 mL (~20 nM).

2.4. LAL activity measurement

The LAL activity was measured by modifying the method reported by Hamilton [7].

For each sample, a 3-mm disk was punched from a DBS. Each punch was placed into a 1.5 mL tube and eluted in 300 μL of water at room temperature for 1 h.

A 0.345 mM substrate solution was prepared from 1.2 mL of 13.3 mM 4-MUP and 42 mL of 100 mM sodium acetate buffer pH 4.0, 1.0%(v/v) Triton X-100 and 3.0 mL of 0.5% (w/v) cardiolipin. Using a black 96-well plate, the enzymatic reactions were performed in the presence and absence of a LAL inhibitor (Lalistat2). Duplicate enzyme reactions and the single blank reactions used for background subtraction were performed for each sample. For the enzyme reaction with the LAL inhibitor, 50 μL of the substrate in buffer solution, 40 μL of the DBS eluate and 10 μL of 30 μM Lalistat2 were combined in a black 96-well plate. For the enzyme reaction without the LAL inhibitor, 50 μL of the substrate in buffer solution, 40 μL of the DBS eluate and 10 μL of water were combined in a black 96-well plate. The plates were sealed with an adhesive aluminum film and incubated in a 37 °C water bath for 24 h. The LAL reactions were terminated using 200 μL of 150 mM EDTA at pH 11.5 (At this point, the solution pH was ~10.9). A standard curve of 0–33.3 μM 4-MU was prepared via serial dilution of a 100 μM aqueous solution of 4-MU (100 μL/well), and 200 μL of 150 mM EDTA at pH 11.5 was added to each well.

The fluorescence of the plates were read immediately with a Corona MTP810 fluorescence microplate reader using a 365-nm excitation filter (FWHM: 6 nm) and a 450-nm emission filter (FWHM: 12 nm). The LAL activity (nmol/punch/h) was calculated by subtracting the enzymatic activity of the inhibited (with Lalistat2) reaction from that of the uninhibited (without Lalistat2) reaction.

The statistical analysis was performed using parametric approaches; comparisons were made using non-repeated measures ANOVA with Student–Newman–Keuls's post-test.

3. Results

3.1. Excitation and emission spectra of 4-MU

Fig. 1 shows the excitation spectra (emission wavelength = 450 nm) of 4-MU at pH values 4.1, 7.1, 8.4 and 10.1. As shown in Fig. 1, the excitation peak of 4-MU was drastically shifted by the solution pH. At pH 4.1, we observed the maximum excitation peak of 4-MU at 320 nm; this peak shifted from 320 nm to 365 nm when the solution pH was increased. In addition, at "acidic pHs (pH 4.1)", there was no peak near

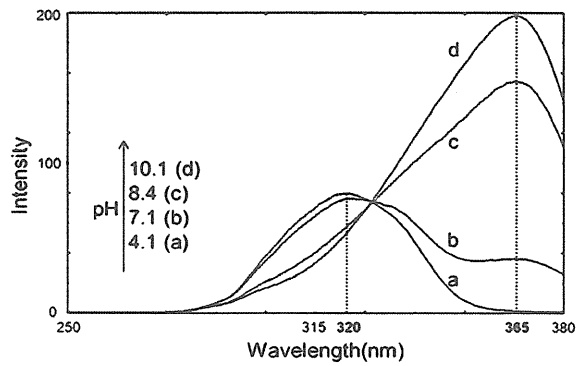

Fig. 1. Excitation spectra (emission wavelength = 450 nm) of 20 nM 4-methylumbelliferone at pH values 4.1 (a), 7.1 (b), 8.4 (c) and 10.1 (d).

Please cite this article as: T. Dairaku, et al., A practical fluorometric assay method to measure lysosomal acid lipase activity in dried blood spots for the screening of choleste..., Mol. Genet. Metab. (2013), http://dx.doi.org/10.1016/j.ymgme.2013.11.003

365 nm. Therefore, even with a 365-nm excitation at "acidic pH (pH 4.1)", 4-MU does not excite.

Fig. 2A shows the emission spectra (excitation wavelength = 365 nm) of 4-MU at pH values 4.1, 7.1, 8.4 and 10.1. As shown in Fig. 2A, the fluorescence intensity slightly increased as the pH increased, drastically changing from pH 7.1 to pH 8.4. At pH 10.1, we observed the maximum emission at 450 nm.

Similar to the well-known chemical properties of 4-MU, at "basic pH (pH 10.1)", the optimal wavelengths used to measure the amount of released 4-MU are 365 nm (excitation) and 450 nm (emission). However, with excitation at 320 nm, the fluorescence intensity slightly decreased as the pH increased and drastically changed from pH 7.1 to pH 8.4 (Fig. 2B). At pH 4.1, we observed the maximum emission peak at 450 nm (Fig. 2B). Fig. 2B revealed that at "acidic pH (pH 4.1)", the optimal wavelengths required to measure the amount of 4-MU released are 320 nm (excitation) and 450 nm (emission).

3.2. LAL activity measurement

The LAL activity in the DBS was measured in 51 normal, 7 obligate carrier and 7 CESD (Fig. 3). The average LAL activities in the DBS from the normal, the obligate carrier and the CESD were 0.68 ± 0.2 (range: 0.3–1.08), 0.21 ± 0.1 (range: 0.11–0.41) and 0.02 ± 0.02 (range: 0–0.06) nmol/punch/h, respectively. There was a significant difference in the LAL activities between the normal, the obligate carrier and the CESD ($P < 0.05$). We tested 8 normal samples for 20 days. The coefficient of variation (CV) value for the normal subjects was 11.9% (within-run) and 19% (day-to-day). The limit of detection was 0.06 nmol/punch/h, and the limit of quantification was 0.2 nmol/punch/h.

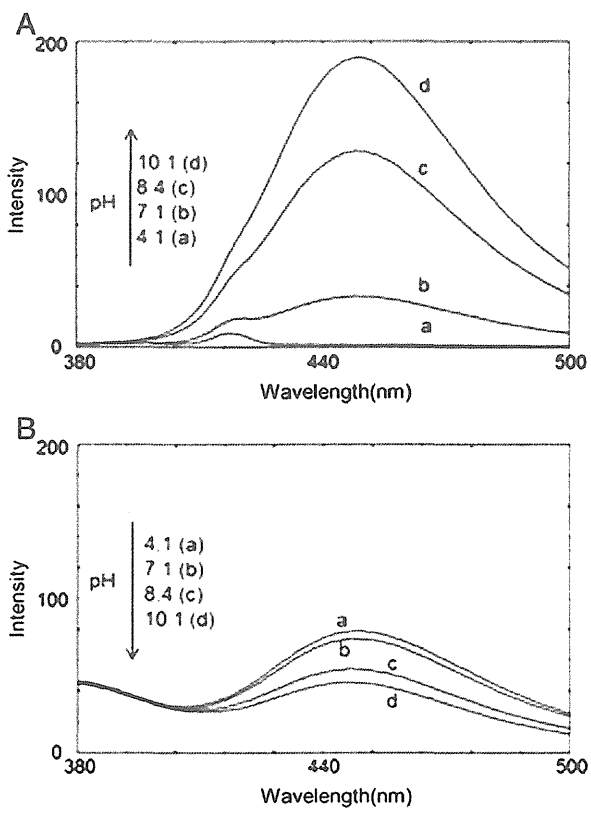

Fig. 2. Emission spectra at excitation wavelength = 365 nm (A) and emission spectra at excitation wavelength = 320 nm (B) of 20 nM 4-methylumbelliferone at pH values 4.1 (a), 7.1 (b), 8.4 (c) and 10.1 (d).

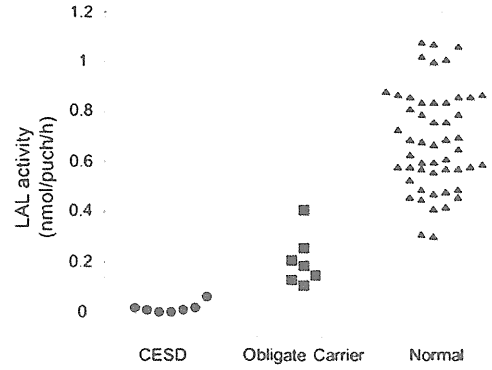

Fig. 3. Comparison of the LAL activity of 51 normal, 7 obligate carriers and 7 CESD samples.

4. Discussion

In this study, we demonstrated that the maximum excitation wavelength required to measure the amount of released 4-MU is different between "basic pH" and "acidic pH" conditions. Based on this fundamental information, we have also developed a revised method for measuring LAL by modifying Hamilton's method [7].

Because the strongest fluorescence intensity of 4-MU was obtained at pH 10 or greater, we used an EDTA solution (pH 11.5) to quench the LAL reaction. Due to the "basic pH" conditions, the fluorescence intensity of the released 4-MU was measured with a fluorescence microplate reader using a 365 nm (FWHM: 6 nm) excitation filter.

Our method has two advantages for screening CESD and WD. First, this technique does not use mercury chloride to quench the LAL reaction. Because mercury chloride is not needed, the screening test for the DBS samples can be carried out safely. Second, we used an excitation filter (365 nm: FWHM; 6 nm) that is commonly used for measuring other lysosome enzymatic activities in DBS. Therefore, screening for CESD and WD could occur at many laboratories using our method. In Hamilton's method, 4-MU was measured under "acidic pH" conditions (~pH 4). To measure the LAL activity under these conditions, we used an excitation filter (e.g., 355 nm: FWHM; ~70 nm) with a large FWHM value, or a band pass excitation filter (e.g., 320 nm: FWHM; ~6 nm).

According to our statistical analysis, the CESD patient group, the obligate carrier group and the normal group could be distinguished, but part of the obligate carrier group and part of the normal group had overlapped. Using DBS, distinguishing the obligate carriers from the normal samples may be difficult, but the DBS of all CESD patients could be detected using our method. Our method can be used to screen newborns for WD and to screen patients with fatty liver/cirrhosis for a high risk of CESD. Furthermore, we can enact early diagnosis and treatment using enzyme replacement therapy in LAL-deficient patients because recombinant enzymes from the egg whites of transgenic *Gallus* are now available [3].

5. Conclusions

Our study demonstrates that a suitable optical filter must be selected for the LAL activity measurement. Based on this finding, we revised a method for measuring the LAL activity by the method published by Hamilton [7]. Our newly developed method for measuring the LAL activity based on the fluorometric analysis of 4-MU will enable safer, more appropriate screening methods for LAL deficiencies (CESD and WD) in high-risk populations or during newborn screening for patients with WD.

Please cite this article as: T. Dairaku, et al., A practical fluorometric assay method to measure lysosomal acid lipase activity in dried blood spots for the screening of choleste..., Mol. Genet. Metab. (2013), http://dx.doi.org/10.1016/j.ymgme.2013.11.003

Acknowledgments

The authors wish to thank Dr. Wiech Norbert (Chemical Tools, LLC) for providing Llistat2. We also wish to acknowledge Dr. Dana Martin, Mr. Yoshio Iijima (Synageva BioPharma) and Dr. John Hamilton for supplying the DBS samples from the CESD patients.

References

[1] C. Aslanidis, S. Ries, P. Fehringer, C. Buchler, H. Klima, G. Schmitz, Genetic and biochemical evidence that CESD and wolman disease are distinguished by residual lysosomal acid lipase activity, Genomics 33 (1996) 85–93.
[2] P. Lohse, S. Maas, P. Lohse, M. Elleder, J.M. Kirk, G.T. Besley, D. Seidel, Compound heterozygosity for a wolman mutation is frequent among patients with cholesteryl ester storage disease, J. Lipid Res. 41 (2000) 23–31.
[3] M. Balwani, C. Breen, G.M. Enns, P.B. Deegan, T. Honzik, S. Jones, J.P. Kane, V. Malinova, R. Sharma, E.O. Stock, V. Valayannopoulos, J.E. Wraith, J. Burg, S. Eckert, E. Schneider, A.G. Quinn, Clinical effect and safety profile of recombinant human lysosomal acid lipase in patients with cholesteryl ester storage disease, Hepatology 58 (2013) 950–957.
[4] G.J. Guy, J. Butterworth, Acid esteraseactivity in culturedskinfibroblasts and amniotic fluid cells using 4-methylumbelliferyl palmitate, Clin. Chim. Acta 84 (1978) 361–371.
[5] P.A. Demirev, Dried blood spots: analysis and applications, Anal. Chem. 85 (2013) 779–789.
[6] G. Civallero, K. Michelin, J. de Mari, M. Viapiana, M. Burin, J.C. Coelho, R. Giugliani, Twelve different enzyme assays on dried-blood filter paper samples for detection of patients with selected inherited lysosomal storage diseases, Clin. Chim. Acta 372 (2006) 98–102.
[7] J. Hamilton, I. Jones, R. Srivastava, P. Galloway, A new method for the measurement of lysosomal acid lipase in dried blood spots using the inhibitor lalistat2, Clin. Chim. Acta 413 (2012) 1207–1210.
[8] A.S. Al-Kady, el-SI. Ahmed, M. Gaber, M.M. Hussein, el-ZM. Ebeid, Kinetics of catalyzed hydrolysis of 4-methylumbelliferyl caprylate (MUCAP) *Salmonella* reagent, Spectrochim. Acta A Mol. Biomol. Spectrosc. 79 (2011) 1540–1545.
[9] M. Nakashima, J.A. Sousa, R.C. Clapp, Spectroscopic species of 4-methylumbelliferone in water and in ethanol, Nature 235 (1972) 16–18.

Please cite this article as: T. Dairaku, et al., A practical fluorometric assay method to measure lysosomal acid lipase activity in dried blood spots for the screening of choleste..., Mol. Genet. Metab. (2013), http://dx.doi.org/10.1016/j.ymgme.2013.11.003

CLINICAL REPORT

AMERICAN JOURNAL OF medical genetics A

Somatic *CTNNB1* Mutation in Hepatoblastoma from a Patient with Simpson–Golabi–Behmel Syndrome and Germline *GPC3* Mutation

Rika Kosaki,[1] Toshiki Takenouchi,[2] Noriko Takeda,[3,4] Masayo Kagami,[5] Kazuhiko Nakabayashi,[6] Kenichiro Hata,[6] and Kenjiro Kosaki[2,7]*

[1]Division of Medical Genetics, National Center for Child Health and Development, Tokyo, Japan

[2]Department of Pediatrics, Keio University School of Medicine, Tokyo, Japan

[3]Department of Surgery, National Center for Child Health and Development, Tokyo, Japan

[4]Department of Surgery, Kitasato University, Kanagawa, Japan

[5]Department of Molecular Endocrinology, National Research Institute of Child Health and Development, Tokyo, Japan

[6]Department of Maternal-Fetal Biology, National Research Institute of Child Health and Development, Tokyo, Japan

[7]Center for Medical Genetics, Keio University School of Medicine, Tokyo, Japan

Manuscript Received: 28 June 2013; Manuscript Accepted: 20 October 2013

Simpson–Golabi–Behmel syndrome is a rare overgrowth syndrome caused by the *GPC3* mutation at Xq26 and is clinically characterized by multiple congenital abnormalities, intellectual disability, pre/postnatal overgrowth, distinctive craniofacial features, macrocephaly, and organomegaly. Although this syndrome is known to be associated with a risk for embryonal tumors, similar to other overgrowth syndromes, the pathogenetic basis of this mode of tumorigenesis remains largely unknown. Here, we report a boy with Simpson-Golabi–Behmel syndrome who had a germline loss-of function mutation in *GPC3*. At 9 months of age, he developed hepatoblastoma. A comparison of exome analysis results for the germline genome and for the tumor genome revealed a somatic mutation, p.Ile35Ser, within the degradation targeting box of β-catenin. The same somatic mutation in *CTNNB1* has been repeatedly reported in hepatoblastoma and other cancers. This finding suggested that the *CTNNB1* mutation in the tumor tissue represents a driver mutation and that both the *GPC3* and the *CTNNB1* mutations contributed to tumorigenesis in a clearly defined sequential manner in the propositus. The current observation of a somatic *CTNNB1* mutation in a hepatoblastoma from a patient with a germline *GPC3* mutation supports the notion that the mutation in *GPC3* may influence one of the initial steps in tumorigenesis and the progression to hepatoblastoma.

Key words: hepatoblastoma; Simpson–Golabi–Behmel syndrome; CTNNB1; GPC3

How to Cite this Article:
Kosaki R, Takenouchi T, Takeda N, Kagami M, Nakabayashi K, Hata K, Kosaki K. 2014. Somatic *CTNNB1* mutation in hepatoblastoma from a patient with Simpson–Golabi–Behmel syndrome and germline GPC3 mutation.
Am J Med Genet Part A 9999:1–5.

INTRODUCTION

Simpson–Golabi–Behmel syndrome (SGBS, OMIM312870) represents an overgrowth syndrome associated with organomegaly and macroglossia accompanied by characteristic external features, such as supernumerary nipples, supernumerary ribs, hypospadias, and cryptorchidism, as well as internal malformations, such as cardiac defects, diaphragmatic hernias, and cystic dysplasia of the kidneys [Cottereau et al., 2013]. SGBS is caused by loss-of-function mutations in the heparan sulphate proteoglycan, glypican 3 gene (*GPC3*) at chromosome Xq26 [Pilia et al., 1996]. The *GPC3* gene encodes an extracellular matrix protein that is expressed during development and that regulates cell proliferation and apoptosis during

Conflict of interest: none.
Grant sponsor: Ministry of Health, Labour and Welfare, Japan the Health and Labour Sciences Research Grant for Research on rare and intractable diseases (Jitsuyoka(Nanbyo)-Ippan-003 & 13).
*Correspondence to:
Kenjiro Kosaki, M.D., Center for Medical Genetics, Keio University School of Medicine 35 Shinanomachi, Shinjuku-ku, Tokyo 160-8582, Japan. E-mail: kkosaki@z3.keio.jp
Article first published online in Wiley Online Library (wileyonlinelibrary.com): 00 Month 2013
DOI 10.1002/ajmg.a.36364

development through the modulation of growth factor action, including that of IGF2 [Gonzalez et al., 1998; Pellegrini et al., 1998].

Patients with SGBS are at an increased risk for the development of embryonal tumors, such as Wilms tumor [Xuan et al., 1994; Hughes-Benzie et al., 1996; Lindsay et al., 1997] and hepatoblastoma [Lapunzina et al., 1998; Li et al., 2001; Buonuomo et al., 2005; Mateos et al., 2013]. In a recent article published in this journal, Mateos et al. [2013] documented a patient with SGBS and a *GPC3* duplication who developed a hepatoblastoma. The pathogenetic basis of the triggering and progression of embryonal tumors in the absence of a functional *GPC3* is currently unknown. Here, we document an infant with a *GPC3* mutation who developed a hepatoblastoma in which the tissue was shown to harbour a *CTNNB1* mutation using exome sequencing. This observation sheds new insight on the stepwise progression of hepatoblastoma.

CLINICAL REPORT

The propositus was born at 41 weeks of gestation as the first child of nonconsanguineous parents. He was delivered by cesarean section. His mother was 35 years old, had a height of 165 cm (+1.3 SD), and had coarse facial features. The father was 54 years old and was healthy. The birth weight of the propositus was 4,068 g (+2.65 SD), his length was 55 cm (+2.8 SD), and his head circumference was 37.5 cm (+2.66 SD). He had a ventricular septal defect that was repaired at the age of 1 month.

At the age of 4 months, his weight was 8.55 kg (+1.61 SD), his length was 68.8 cm (+1.71 SD), and his head circumference was 43.8 cm (+1.6 SD). He had an upturned bulbous nose, a wide nasal bridge, apparent hypertelorism, macrostomia, macroglossia, a midline grooved tongue, a right accessory nipple, and a short webbed neck. His hands were broad, and he had right index fingernail hypoplasia. Based on these clinical features, he was diagnosed as having SGBS (Fig. 1A). Regular surveillance was started to screen for the possible development of abdominal tumors, including hepatoblastoma and Wilms tumor. A cystic lesion was detected in the hepatic parenchyma at 9 months during an abdominal ultrasound examination. An abdominal CT scan revealed a 45 mm × 35 mm × 35 mm heterogeneously enhancing mass localized in S4 that was classified as PRETEXT stage III (Fig 1B,C). The patient's serum α-fetoprotein was elevated to 658 ng/ml. A fine needle biopsy led to a pathological diagnosis of hepatoblastoma. After chemotherapy with cisplatin and tetrahydropyranyladriamycin, the residual mass was surgically removed at the age of 14 months. At the age of 2 years, he continued to demonstrate overgrowth, with a weight of 17.1 kg (+4.58 SD) and a length of 95.7 cm (+3.4 SD).

MOLECULAR INVESTIGATION

Informed consent from the parents and approval from the institutional review board were obtained for the molecular studies. We first performed Sanger sequencing of the *GPC3* gene using DNA obtained from a peripheral blood sample of the propositus. A c.1159C > T, p.Arg387X mutation was identified, confirming the diagnosis of SGBS. Next, we obtained DNA from the hepatoblastoma tissue resected at the time of biopsy. A matched non-tumor

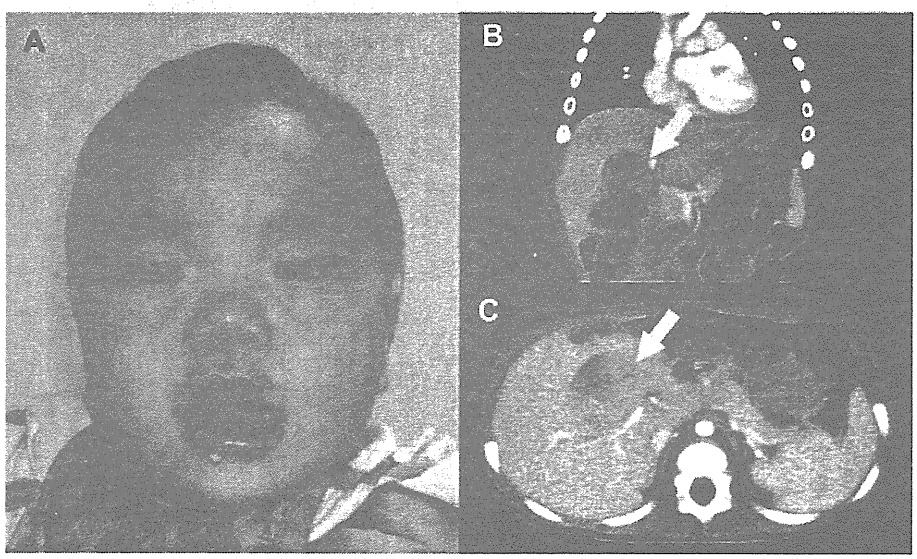

FIG. 1. The characteristic facial features and hepatoblastoma in the propositus. A: Note that the facial features of the propositus included upturned bulbous nose, a wide nasal bridge, apparent hypertelorism, macrostomia, macroglossia, and a midline grooved tongue. B and C: Coronal (B) and axial (C) slices of magnetic resonance imaging at 9 months of age showed a well-demarcated heterogeneously enhancing mass, measuring 45 mm × 35 mm × 35 mm, in S4 of the liver (yellow arrows).

peripheral blood DNA sample was also obtained. Whole-exome sequencing was performed for both DNA samples. Massive parallel sequencing on an Illumina HiSEQ platform yielded ~11 gigabases per sample, with a mean coverage of 114-fold across 54 Mb of targeted coding regions (SureSelectXT2 Human All Exon V4; Agilent Technologies, Santa Clara, CA) for each sample. The sequence reads were aligned to the reference genome assemblies (hg19) using BWA [Li and Durbin, 2009]. Local realignment around the insertions/deletions and base quality score recalibration were performed using the Genome Analysis Tool Kit software [McKenna et al., 2010], with duplicate reads removed using Picard. On average, 73% of the coding bases were covered in sufficient depth in both the tumor and the matched normal samples to allow for confident mutation detection.

MuTect version 1.14 [Cibulskis et al., 2013] was used for comparison of the exome data derived from hepatoblastoma and that derived from the peripheral blood. The default parameters were used except that max_alt_alleles_in_normal_count and minimum_mutation_cell_fraction were set to 0 and 0.1, respectively. The Mutect program detected seventy mutations as a somatic change. These 70 mutations were annotated by the program SnpEff [Cingolani et al., 2012] and classified into the following classes of mutations: non-synonymous coding, non-synonymous start, splice site acceptor, splice site donor, start lost, stop gained, and stop lost. A mutation c.104T > G, p.Ile35Ser (NM_00904) was identified at exon 3 of the *CTNNB1* that encodes β-catenin, and was the only remaining somatic mutation through the filtering process described above. This alteration was confirmed using Sanger sequencing (Fig. 2). An analysis of the reads at the mutant position after the removal of duplicated reads revealed that 72 out of 171 reads were mutant.

Mutations within a targeting box are known to lead to the accumulation of intracytoplasmic and nuclear β-catenin protein [Koch et al., 1999; Purcell et al., 2011]. The catalog of somatic mutations in cancer (COSMIC) version 64 database contained 28 instances of samples containing the somatic mutation p.Ile35Ser in *CTNNB1* under the query conditions "confirmed somatic" or "previously reported"; "tumor sample, not cultured"; and "not reported as polymorphism in the 1,000 genome projects". Out of the 29 samples, 21 originated from the liver, 2 from soft tissue, and 1 each from the endometrium, pituitary, thymus, central nervous system, and lung. Hence, most of, if not all, the samples with p.Ile35Ser were derived from the liver. Among the 21 samples, 4 samples were specifically labeled as hepatoblastoma samples; in the remaining samples, the patient's age was not mentioned, and the clinical distinction between hepatocellular carcinoma versus hepatoblastoma was not mentioned. Furthermore, a literature review on *CTNNB1* mutation analyses in hepatoblastomas in patients without multiple malformation syndromes indicated that at least five patients carried the c.104T > G, p.Ile35Ser mutation [Takayasu et al., 2001; Cairo et al., 2008; Lopez-Terrada et al., 2009; Purcell et al., 2011; Chavan et al., 2012]. The article by Takayasu et al. was not catalogued in the COSMIC database.

DISCUSSION

Through Bayesian comparison of the exome data between the germline genome and the tumor genome, we identified a somatic *CTNNB1* mutation, p.Ile35Ser, within the degradation targeting box of β-catenin in the hepatoblastoma tissue of a patient with an overgrowth syndrome, SGBS, who had a loss-of-function mutation in the *GPC3* gene.

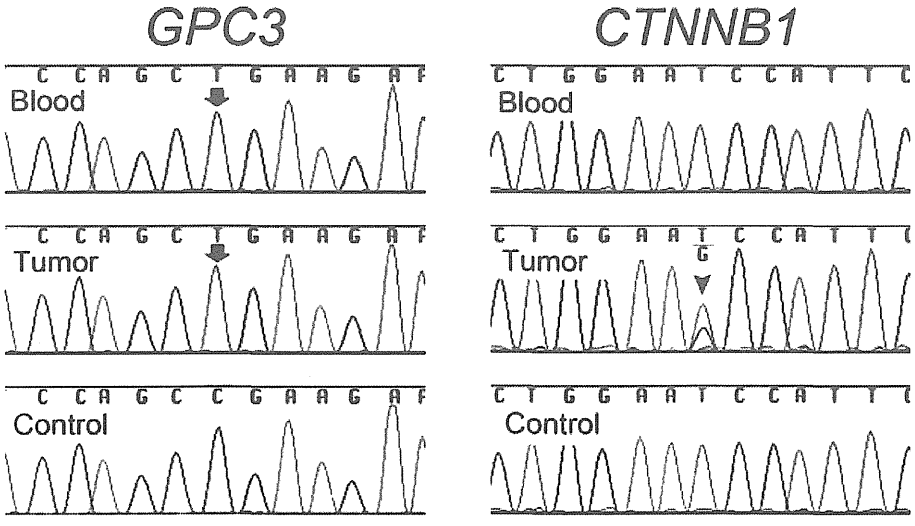

FIG. 2. Partial DNA sequences, including the sequences containing the mutations in the *GPC3* and *CTNNB1* genes. In a blood sample, a hemizygous mutation, c.1159C > T (top arrow), was identified in *GPC3*, but no mutations were identified in *CTNNB1*. In tumor tissue, a hemizygous mutation, c.1159C > T (bottom arrow), was identified in *GPC3* and a heterozygous mutation, c.104T > G (arrowhead), was identified in *CTNNB1*. The control shows a normal peripheral blood sample from a normal individual.

In general, the mutations identified in tumor tissue can be classified into two groups [Burgess, 2013]: "Driver mutations" that are directly involved in tumorigenesis followed by tumor progression, and "passenger mutations" that are not responsible for tumorigenesis or tumor progression but are by-products of genomic instability in tumor cells and are biologically neutral. A distinguishing feature of driver mutations is the recurrent appearance of the same somatic mutation in different individuals. Since the p.Ile35Ser mutation has been reported at least five times in hepatoblastomas [Takayasu et al., 2001; Cairo et al., 2008; Lopez-Terrada et al., 2009; Purcell et al., 2011; Chavan et al., 2012] and 17 times in samples from non-hepatoblastoma liver tumors, including hepatocellular carcinoma, it is reasonable to assume that the p.Ile35Ser *CTNNB1* mutation in the tumor tissue from the propositus represents a driver mutation.

The software MuTect has been shown to be efficient at detecting somatic mutations in a relatively small percentage (i.e., <10%) of tumor cells in a normal tissue background. Hence, the chance of missing mutations in other genes that are present in a subset of the cells in the tumor tissue is unlikely to be very high. Nevertheless, the classes of mutations that have been missed could include but are not limited to: (1) mutations in low coverage areas; (2) mutations in non-coding portions of the genome, such as in non-coding RNAs or regulatory elements; and (3) epigenetic changes that are undetectable using exome sequencing.

The identification of the *CTNNB1* mutation in a patient with SGBS sheds new light on the pathogenesis of hepatoblastoma: *CTNNB1* mutations within a targeting box, in which the propositus' p.Ile35Ser mutation resided, are known to lead to the accumulation of intracytoplasmic and nuclear β-catenin protein and to potentiate canonical Wnt/β-catenin signaling [Koch et al., 1999; Purcell et al., 2011]. Of note, the loss of Gpc3 leads to the activation of canonical Wnt/β-catenin signaling in *Gpc3*-knockout mice [Song et al., 2005]. If this finding is extrapolated to humans, the *GPC3* loss-of-function mutation could have exerted an additive effect on the potentiation of canonical Wnt/β-catenin signaling by the *CTNNB1* mutation. Given the fact that the propositus harbored a germline *GPC3* mutation and that the tumor harbored a somatic *CTNNB1* mutation together with the *GPC3* mutation, *GPC3* and *CTNNB1* apparently contributed to tumorigenesis in a clearly defined sequential manner, at least in the propositus. Whether mutations in *GPC3* and *CTNNB1* must occur in this specific sequence, and not vice versa, remains uncertain. Somatic loss-of-function mutations in *GPC3* have been reported in tumor tissues with various origins, including the lung (6/18), kidney (3/18), endometrium (3/18), large intestine (2/18), breast (1/18), prostate (1/18), and skin (2/18), but not in the liver according to the COSMIC database, version 66 [Forbes et al., 2011], and a search performed under the query conditions "confirmed somatic" or "previously reported"; "tumor sample, not cultured"; and "not reported" as polymorphism in the 1,000 genome projects. Hence, mutations in *GPC3* are unlikely to yield a liver-tumor-specific susceptibility to tumorigenesis or tumor progression.

From an etiological standpoint, SGBS and another prototypic overgrowth syndrome, Beckwith–Wiedemann syndrome (BWS, OMIM130650), share a key fetal growth accelerator, IGF2: the overproduction of IGF2 in BWS and the lack of an anchoring action of IGF2 by the extracellular matrix protein GPC3 in SGBS both promote fetal growth. Patients with BWS are known to have an increased susceptibility to hepatoblastoma, similar to patients with SGBS [Fukuzawa et al., 2003]. Further elucidation of the role of the *CTNNB1* mutation in hepatoblastomas in patients with BWS is warranted. Similarly, the likely role of *CTNNB1* mutation in the pathogenesis of Wilms tumor in both SGBS and BWS should be explored, together with the potential role of *GPC3* mutation in isolated hepatoblastomas.

In summary, we here document a somatic *CTNNB1* mutation in a hepatoblastoma from a patient with SGBS and a germline *GPC3* mutation. The current observation supports the notion that a mutation in *GPC3* may represent an initial step in the tumorigenesis and progression of hepatoblastoma.

ACKNOWLEDGMENTS

This work was supported by the Health and Labour Sciences Research Grant for Research on rare and intractable diseases (Jitsuyoka(Nanbyo)-Ippan-003) and Research on Applying Health Technology (H23-013) from the Ministry of Health, Labour and Welfare, Japan. We thank Ms. Yumi Obayashi for her technical assistance in article preparation.

REFERENCES

Buonuomo PS, Ruggiero A, Vasta I, Attina G, Riccardi R, Zampino G. 2005. Second case of hepatoblastoma in a young patient with Simpson-Golabi-Behmel syndrome. Pediatr Hematol Oncol 22:623–628.

Burgess DJ. 2013. Tumour evolution: Weighed down by passengers? Nat Rev Cancer 13:219.

Cairo S, Armengol C, De Reynies A, Wei Y, Thomas E, Renard CA, Goga A, Balakrishnan A, Semeraro M, Gresh L, Pontoglio M, Strick-Marchand H, Levillayer F, Nouet Y, Rickman D, Gauthier F, Branchereau S, Brugieres L, Laithier V, Bouvier R, Boman F, Basso G, Michiels JF, Hofman P, Arbez-Gindre F, Jouan H, Rousselet-Chapeau MC, Berrebi D, Marcellin L, Plenat F, Zachar D, Joubert M, Selves J, Pasquier D, Bioulac-Sage P, Grotzer M, Childs M, Fabre M, Buendia MA. 2008. Hepatic stem-like phenotype and interplay of Wnt/beta-catenin and Myc signaling in aggressive childhood liver cancer. Cancer Cell 14:471–484.

Chavan RS, Patel KU, Roy A, Thompson PA, Chintagumpala M, Goss JA, Nuchtern JG, Finegold MJ, Parsons DW, Lopez-Terrada DH. 2012. Mutations of PTCH1, MLL2, and MLL3 are not frequent events in hepatoblastoma. Pediatr Blood Cancer 58:1006–1007.

Cibulskis K, Lawrence MS, Carter SL, Sivachenko A, Jaffe D, Sougnez C, Gabriel S, Meyerson M, Lander ES, Getz G., 2013. Sensitive detection of somatic point mutations in impure and heterogeneous cancer samples. Nat Biotechnol 31:213–219.

Cingolani P, Platts A, Wang le L, Coon M, Nguyen T, Wang L, Land SJ, Lu X, Ruden DM. 2012. A program for annotating and predicting the effects of single nucleotide polymorphisms, SnpEff: SNPs in the genome of Drosophila melanogaster strain w1118; iso-2; iso-3. Fly (Austin) 6:80–92.

Cottereau E, Mortemousque I, Moizard MP, Burglen L, Lacombe D, Gilbert-Dussardier B, Sigaudy S, Boute O, David A, Faivre-Olivier L, Amiel J, Robertson R, Viana Ramos F, Bieth E, Odent S, Demeer B, Mathieu M, Gaillard D, Van Maldergem L, Baujat G, Maystadt I, Heron D, Verloes A, Philip N, Cormier-Daire V, Froute MF, Pinson L, Blanchet P, Sarda P, Willems M, Jacquinet A, Ratbi I, van den Ende J, Lackmy-Port Lis M, Goldenberg A, Bonneau D, Rossignol S, Toutain A. 2013.

Phenotypic spectrum of simpson-golabi-behmel syndrome in a series of 42 cases with a mutation in GPC3 and review of the literature. Am J Med Genet C Semin Med Genet 163C:92–105.

Forbes SA, Bindal N, Bamford S, Cole C, Kok CY, Beare D, Jia M, Shepherd R, Leung K, Menzies A, Teague JW, Campbell PJ, Stratton MR, Futreal PA. 2011. COSMIC: Mining complete cancer genomes in the catalogue of somatic mutations in cancer. Nucleic Acids Res 39:D945–D950.

Fukuzawa R, Hata J, Hayashi Y, Ikeda H, Reeve AE. 2003. Beckwith-Wiedemann syndrome-associated hepatoblastoma: Wnt signal activation occurs later in tumorigenesis in patients with 11p15.5 uniparental disomy. Pediatr Dev Pathol 6:299–306.

Gonzalez AD, Kaya M, Shi W, Song H, Testa JR, Penn LZ, Filmus J. 1998. OCI-5/GPC3, a glypican encoded by a gene that is mutated in the Simpson-Golabi-Behmel overgrowth syndrome, induces apoptosis in a cell line-specific manner. J Cell Biol 141:1407–1414.

Hughes-Benzie RM, Pilia G, Xuan JY, Hunter AG, Chen E, Golabi M, Hurst JA, Kobori J, Marymee K, Pagon RA, Punnett HH, Schelley S, Tolmie JL, Wohlferd MM, Grossman T, Schlessinger D, MacKenzie AE. 1996. Simpson-Golabi-Behmel syndrome: Genotype/phenotype analysis of 18 affected males from 7 unrelated families. Am J Med Genet 66:227–234.

Koch A, Denkhaus D, Albrecht S, Leuschner I, von Schweinitz D, Pietsch T. 1999. Childhood hepatoblastomas frequently carry a mutated degradation targeting box of the beta-catenin gene. Cancer Res 59:269–273.

Lapunzina P, Badia I, Galoppo C, De Matteo E, Silberman P, Tello A, Grichener J, Hughes-Benzie R. 1998. A patient with Simpson-Golabi-Behmel syndrome and hepatocellular carcinoma. J Med Genet 35:153–156.

Li H, Durbin R. 2009. Fast and accurate short read alignment with Burrows-Wheeler transform. Bioinformatics 25:1754–1760.

Li M, Shuman C, Fei YL, Cutiongco E, Bender HA, Stevens C, Wilkins-Haug L, Day-Salvatore D, Yong SL, Geraghty MT, Squire J, Weksberg R. 2001. GPC3 mutation analysis in a spectrum of patients with overgrowth expands the phenotype of Simpson-Golabi-Behmel syndrome. Am J Med Genet 102:161–168.

Lindsay S, Ireland M, O'Brien O, Clayton-Smith J, Hurst JA, Mann J, Cole T, Sampson J, Slaney S, Schlessinger D, Burn J, Pilia G. 1997. Large scale deletions in the GPC3 gene may account for a minority of cases of Simpson-Golabi-Behmel syndrome. J Med Genet 34:480–483.

Lopez-Terrada D, Gunaratne PH, Adesina AM, Pulliam J, Hoang DM, Nguyen Y, Mistretta TA, Margolin J, Finegold MJ. 2009. Histologic subtypes of hepatoblastoma are characterized by differential canonical Wnt and Notch pathway activation in DLK+ precursors. Hum Pathol 40:783–794.

Mateos ME, Beyer K, Lopez-Laso E, Siles JL, Perez-Navero JL, Pena MJ, Guzman J, Matas J. 2013. Simpson-golabi-behmel syndrome type 1 and hepatoblastoma in a patient with a novel exon 2-4 duplication of the GPC3 gene. Am J Med Genet Part A 161A:1091–1095.

McKenna A, Hanna M, Banks E, Sivachenko A, Cibulskis K, Kernytsky A, Garimella K, Altshuler D, Gabriel S, Daly M, DePristo MA. 2010. The genome analysis toolkit: A Mapreduce framework for analyzing next-generation DNA sequencing data. Genome Res 20:1297–1303.

Pellegrini M, Pilia G, Pantano S, Lucchini F, Uda M, Fumi M, Cao A, Schlessinger D, Forabosco A. 1998. Gpc3 expression correlates with the phenotype of the Simpson-Golabi-Behmel syndrome. Dev Dyn 213:431–439.

Pilia G, Hughes-Benzie RM, MacKenzie A, Baybayan P, Chen EY, Huber R, Neri G, Cao A, Forabosco A, Schlessinger D. 1996. Mutations in GPC3, a glypican gene, cause the Simpson-Golabi-Behmel overgrowth syndrome. Nat Genet 12:241–247.

Purcell R, Childs M, Maibach R, Miles C, Turner C, Zimmermann A, Sullivan M. 2011. HGF/c-Met related activation of beta-catenin in hepatoblastoma. J Exp Clin Cancer Res 30:96.

Song HH, Shi W, Xiang YY, Filmus J. 2005. The loss of glypican-3 induces alterations in Wnt signaling. J Biol Chem 280:2116–2125.

Takayasu H, Horie H, Hiyama E, Matsunaga T, Hayashi Y, Watanabe Y, Suita S, Kaneko M, Sasaki F, Hashizume K, Ozaki T, Furuuchi K, Tada M, Ohnuma N, Nakagawara A. 2001. Frequent deletions and mutations of the beta-catenin gene are associated with overexpression of cyclin D1 and fibronectin and poorly differentiated histology in childhood hepatoblastoma. Clin Cancer Res 7:901–908.

Xuan JY, Besner A, Ireland M, Hughes-Benzie RM, MacKenzie AE. 1994. Mapping of Simpson-Golabi-Behmel syndrome to Xq25-q27. Hum Mol Genet 3:133–137.

Differentiation of Monkey Embryonic Stem Cells to Hepatocytes by Feeder-Free Dispersion Culture and Expression Analyses of Cytochrome P450 Enzymes Responsible for Drug Metabolism

Junya Maruyama,[a] Tamihide Matsunaga,[b] Satoshi Yamaori,[a] Sakae Sakamoto,[c] Noboru Kamada,[c] Katsunori Nakamura,[b] Shinji Kikuchi,[c] and Shigeru Ohmori*[,a]

[a] *Department of Pharmacy, Shinshu University Hospital; 3–1–1 Asahi, Matsumoto 390–8621, Japan:* [b] *Graduate School of Pharmaceutical Sciences, Nagoya City University; 3–1 Tanabe-dori, Mizuho-ku, Nagoya 467–8603, Japan: and* [c] *Kissei Pharmaceutical Co., Ltd.; 4365–1 Kashiwabara, Hotaka, Azumino 399-8304, Japan.*
Received October 3, 2012; accepted November 15, 2012; advance publication released online December 8, 2012

We reported previously that monkey embryonic stem cells (ESCs) were differentiated into hepatocytes by formation of embryoid bodies (EBs). However, this EB formation method is not always efficient for assays using a large number of samples simultaneously. A dispersion culture system, one of the differentiation methods without EB formation, is able to more efficiently provide a large number of feeder-free undifferentiated cells. A previous study demonstrated the effectiveness of the Rho-associated kinase inhibitor Y-27632 for feeder-free dispersion culture and induction of differentiation of monkey ESCs into neural cells. In the present study, the induction of differentiation of cynomolgus monkey ESCs (cmESCs) into hepatocytes was performed by the dispersion culture method, and the expression and drug inducibility of cytochrome P450 (CYP) enzymes in these hepatocytes were examined. The cmESCs were successfully differentiated into hepatocytes under feeder-free dispersion culture conditions supplemented with Y-27632. The hepatocytes differentiated from cmESCs expressed the mRNAs for three hepatocyte marker genes (α-fetoprotein, albumin, CYP7A1) and several CYP enzymes, as measured by real-time polymerase chain reaction. In particular, the basal expression of cmCYP3A4 (3A8) in these hepatocytes was detected at mRNA and enzyme activity (testosterone 6β-hydroxylation) levels. Furthermore, the expression and activity of cmCYP3A4 (3A8) were significantly upregulated by rifampicin. These results indicated the effectiveness of Y-27632 supplementation for feeder-free dispersed culture and induction of differentiation into hepatocytes, and the expression of functional CYP enzyme(s) in cmESC-derived hepatic cells.

Key words embryonic stem cell; differentiation; hepatocyte; monkey; cytochrome P450; feeder-free dispersed culture

Investigation of drug metabolism with human hepatocytes is important in the early stages of drug development. However, primary human hepatocytes are short-lived and cannot be maintained in culture over the long term. In addition, there are large donor-dependent variations in drug metabolism. On the other hand, human embryonic stem cells (ESCs) are able to replicate infinitely and differentiate into various types of somatic cells including germ cells.[1] Thus, they represent an attractive source to provide large numbers of cells that can be utilized for the development of candidate drug-screening strategies in place of primary cells.[2] However, ethical and legal restrictions have limited the availability of human ESCs. The phenotype of human ESCs is known to closely resemble that of monkey ESCs but not mouse ESCs with regard to morphology, leukemia inhibitory factor responsiveness, gene expression profiles, and some disease models.[1,3–6] Thus, monkey ESCs are a more suitable model for preclinical research of drug development. In particular, hepatocytes derived from monkey ESCs may be useful for pharmacokinetic studies, such as investigation of drug–drug interactions and the inducibility of drug-metabolizing enzymes, including cytochrome P450 (CYP).

We reported previously that monkey ESCs were successfully differentiated into hepatocytes by the formation of embryoid bodies (EBs) and treatment with specific growth factors and cytokines critical for hepatic differentiation.[7] EBs can mimic the inductive microenvironment required for liver organogenesis[8–10] and develop into many different cell types in culture. However, this EB formation method is not always appropriate for assays with large numbers of samples, such as high-throughput screening, because the formation of EBs is inefficient. A dispersion culture system, one of the differentiation methods without EB formation, can more efficiently provide a large number of feeder-free undifferentiated cells. The Rho-associated kinase (ROCK) inhibitor Y-27632 enables expansion from single-cell culture of human ESCs under dispersion culture conditions because the ROCK inhibitor markedly reduces dissociation-induced apoptosis of human ESCs.[11] Furthermore, Takehara *et al.*[12] conducted direct neural stem cell induction from cynomolgus monkey (*Macaca fascicularis*) ESCs (cmESCs) using Y-27632 and demonstrated the effectiveness of Y-27632 supplementation for feeder-free culture and induction of differentiation. However, it is not clear whether this dispersion culture method is effective for differentiation of monkey ESCs into hepatocytes.

In the present study, we carried out induction of hepatocyte differentiation from cmESCs by the dispersion culture method and examined expression and drug inducibility of CYP in the differentiated cells.

MATERIALS AND METHODS

Materials Growth Factor Reduced BD Matrigel Matrix (Matrigel reduced) was obtained from BD Biosciences

The authors declare no conflict of interest.

* To whom correspondence should be addressed. e-mail: somori@shinshu-u.ac.jp

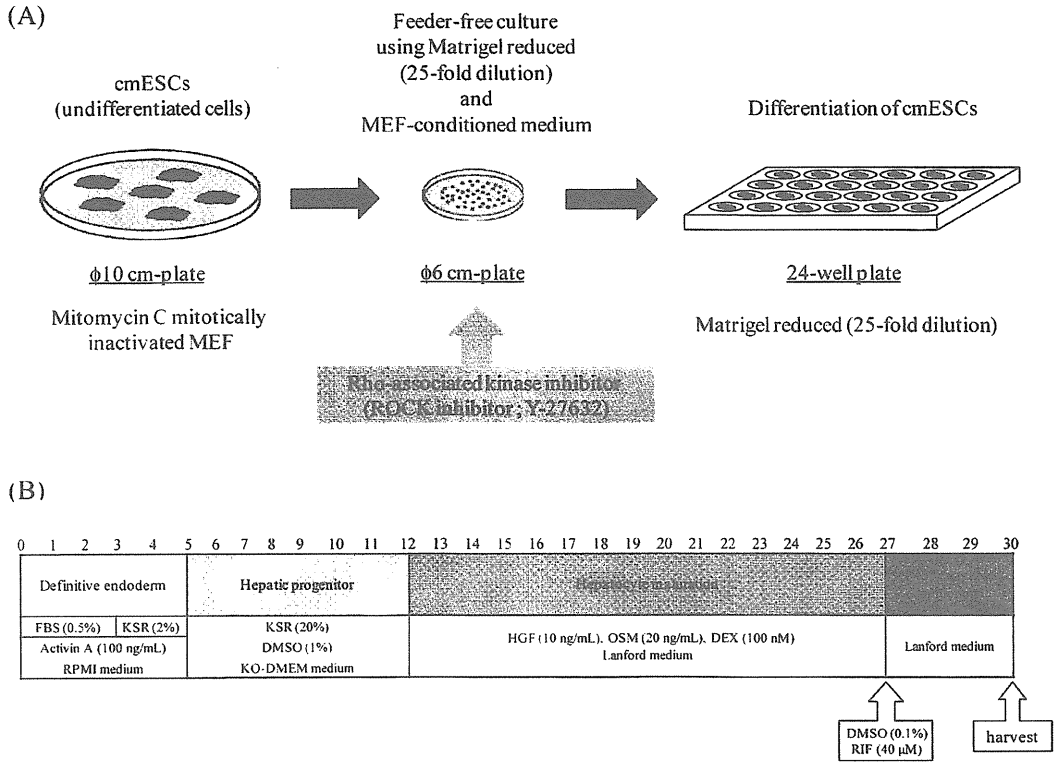

Fig. 1. Scheme of *in Vitro* Differentiation of cmESCs into Hepatocytes

(A) Illustration of the feeder-free dispersion culture of undifferentiated cmESCs. (B) Schematic procedure of differentiation of cmESCs into hepatocytes and drug treatment.

(Bedford, MA, U.S.A.); mitomycin C, Dulbecco's modified Eagle's medium (DMEM), William's E medium with GlutaMAX without phenol red, MEM non-essential amino acid solution (100×), and 6β-hydroxytestosterone from Sigma (St. Louis, MO, U.S.A.); murine embryonic fibroblasts (MEF) from Oriental Yeast (Tokyo, Japan); RPMI1640 medium supplemented with GlutaMAX, KnockOut™ DMEM, KnockOut Serum Replacement (KSR), minimum essential medium (MEM), L-glutamine, 0.25% (w/v) trypsin-ethylenediaminetetraacetic acid (EDTA), and SuperScript™ III First-Strand Synthesis System for reverse transcription-polymerase chain reaction (RT-PCR) from Invitrogen Life Technologies (Carlsbad, CA, U.S.A.); fetal bovine serum (FBS) from Equitech-Bio, Inc. (Kerrville, TX, U.S.A.); recombinant human activin A and recombinant human hepatocyte growth factor (HGF) from Funakoshi Co., Ltd. (Tokyo, Japan); modified Lanford medium from Charles River Laboratories Japan Inc. (Yokohama, Japan); recombinant human basic fibroblast growth factor (bFGF), Y-27632, oncostatin M (OSM), dexamethasone (DEX), rifampicin (RIF), testosterone, and dimethyl sulfoxide (DMSO) from Wako Pure Chemicals (Osaka, Japan); [$^2H_7$]6β-hydroxytestosterone from BD Gentest (Franklin Lakes, NJ, U.S.A.); illustra RNAspin Mini RNA Isolation kit from GE Healthcare (Tokyo, Japan); SYBR® Green real-time PCR Master Mix from TaKaRa Bio (Otsu, Japan). All other reagents used were of the highest quality available.

ESC Culture and Differentiation The cmESCs (CMK6) were generously provided by Tanabe Seiyaku Co., Ltd. (Osaka, Japan)[4] and maintained according to the method reported previously[7] except that recombinant human bFGF was added to ES medium. Feeder-free dispersed culture was carried out as follows (Fig. 1A). The cmESCs were cultured in the presence of 10 μM Y-27632 for 1 h before detaching the cells from the feeder layer. After detachment of the cmESCs, contaminating MEF were removed by incubating the cell suspension on gelatin-coated plates (BD Falcon, Franklin Lakes, NJ, U.S.A.) at 37°C for 2 h. The cmESC clumps were recovered from the suspension by centrifugation, incubated in 0.25% (w/v) trypsin-EDTA solution at 37°C for 5 min, and dissociated into single cells by pipetting. The cells were passed through a Cell Strainer (40 μm mesh; BD Falcon) and seeded onto culture plates 6 cm in diameter (BD Falcon) coated with Matrigel reduced (25-fold dilution). The cmESCs were cultured in medium conditioned by contact with MEF with 4 ng/mL recombinant human bFGF and 10 μM Y-27632 for the first 24 h. The medium was changed for MEF-conditioned medium for cmESCs without Y-27632.

When cmESCs reached approximately 70% confluence, differentiation was initiated by replacing RPMI1640 medium supplemented with GlutaMax containing 0.5% FBS and 100 ng/mL activin A (Fig. 1B). After 72 h, the medium was changed to RPMI1640 medium supplemented with GlutaMax containing 2% KSR and 100 ng/mL activin A, and culture was continued for 48 h. The cells were passaged onto 24-well plates coated with Matrigel reduced (25-fold dilution) and cultured in KnockOut™ DMEM containing 20% KSR, 1 mM L-glutamine, 1% MEM nonessential amino acids, and 1% DMSO for 7 d. Finally, the cells were cultured in modified Lanford medium containing 10 ng/mL HGF, 20 ng/mL OSM, and 100 nM DEX. The medium was changed daily during differentiation.

Table 1. Primers Used for Real-Time PCR Analysis

Genes	Forward primer (5′–3′)	Reverse primer (5′–3′)	Product (bp)
AFP	ACTATTGGCCTGTGGTGAGG	CACCCTGAGCTTGACACAGA	224
ALB	CTTCCTGGGCATGTTTTTGT	GGCTCTTCCACAAGAGGTTG	177
CYP1A1	CTAGACACAGTGATTGGCAGGTC	GGTTGACCCATAGCTTCTGGTCA	232
cmCYP2B6 (2B30)	GGGGCATTGAAGAAGAATGA	ATTTTGCCCACACCACTCTC	188
cmCYP2C9 (2C43)	TGATTCCCAAGGGTACAACC	AAATTGCCACCTTCATCCAG	118
cmCYP2D6 (2D17)	AGATCGACGACGTGATAGGG	GTCCCCTTAGGGATGAGGAA	178
cmCYP3A4 (3A8)	CCAAGAAGCTTTTAAGATTTGATTTC	ATCTACTCGGTGCTTTTGTGTA	191
cmCYP3A5 (3A66)	TTTGCCCAATAAGGCACCTG	GGTTGGAATCACCACCATTG	181
CYP7A1	ATTTGGTGCCAATCCTCTTG	CATCCTTTGGGTCAATGCTT	215
AhR	ACTCCACTTCAGCCACCATC	CTCGTGCACAGTTCTGCTTC	146
PXR	AAGGATGCAAGGGCTTTTTC	TTCTTCATGCCGCTCTCC	151
GAPDH	GTCAGTGGACCTGACCT	TGCTGTAGCCAAATTCGTTG	245

AFP, α-fetoprotein; ALB, albumin; AhR, aryl hydrocarbon receptor; PXR, pregnane X receptor; GADPH, glyceraldehyde-3-phosphate dehydrogenase

Drug Treatment To clarify the effects of RIF on expression of CYP, cmESC-derived hepatocytes were treated with 40 μM RIF for 72 h (Fig. 1B). The compound was dissolved in DMSO, which was added to the modified Lanford medium at a final concentration of 0.1%.

Primary Hepatocyte Culture Primary cynomolgus monkey hepatocytes (primary cmHCs, Batch HEP 18605) were obtained from BIOPREDIC International (Renes, France). The primary cmHCs were thawed according to the manufacturer's instructions. Briefly, the primary cmHCs were cultured on 24-well plates (BD Falcon) in William's E medium with GlutaMax without phenol red for 72 h, and the medium was changed daily.

Real-time PCR Analysis Total RNA was isolated from the cells and the liver of an adult male monkey (Ina Research Inc., Ina, Japan) using the illustra RNAspin Mini RNA Isolation kit according to the manufacturer's protocol. First-strand cDNA was generated from 5 μg of total RNA. Reverse transcription reaction was performed using the SuperScript™ III First-Strand Synthesis System for RT-PCR in accordance with the manufacturer's instructions. For detection of mRNA expression levels, CYP mRNAs were analyzed by SYBR® Green real-time quantitative PCR. All PCR procedures were performed using the ABI Prism 7300 Real-time PCR System (Applied Biosystems, Foster City, CA, U.S.A.). PCR was performed in a mixture consisting of 10 μL of SYBR® Green real-time PCR Master Mix, 0.4 μL of 10 μM forward and reverse primers, 0.4 μL of dye, 7.8 μL of water, and 1 μL template cDNA in a total of 20 μL. The primers used are summarized in Table 1. The levels of these mRNAs were normalized relative to that of glyceraldehyde-3-phosphate dehydrogenase (GAPDH) mRNA.

Measurement of Cellular Activity of Testosterone 6β-Hydroxylation Following drug treatment, cmESC-derived hepatocytes were incubated with 100 μM testosterone in modified Lanford medium for 6 h. On the other hand, primary cmHCs were incubated with 100 μM testosterone in MEM for 6 h. After incubation, each medium was collected and 6β-hydroxytestosterone was measured by LC-MS/MS under the conditions described below.

Instrument An Agilent 1100 series HPLC system (Agilent Technologies, Waldbronn, Germany) consisting of a binary pump, a degasser linked to a CTC HTS PAL New Wash System Autosampler (AMR Inc., Tokyo, Japan) was used.

Table 2. Timetable for HPLC

Time (min)	Solvent A (%)	Solvent B (%)
0	10	90
3	10	90
6	90	10
9	90	10
9.1	10	90
16	10	90

Solvents A: 10 mM ammonium acetate in water. Solvents B: 0.1% formic acid in methanol.

Mass spectrometry was performed on an API 4000 triple quadruple instrument (Applied Biosystems/Sciex, Foster City, CA, U.S.A.) equipped with a TurboIonSpray® electrospray ionization (ESI) interface. Data processing was performed with the Analyst 1.4.2 software package (Applied Biosystems/Sciex).

Chromatographic Conditions Chromatographic separation was performed on a reversed-phase CAPCELL PAK C18 MG III column (50×4.6 mm i.d., 5 μm; Shiseido Co., Inc., Tokyo, Japan). The column temperature was kept constant at 40°C. The mobile phase consisted of a mixture of 10 mM ammonium acetate in water (A) with 0.1% formic acid in methanol (B) and was delivered at a flow rate of 0.5 mL/min. A stepwise gradient was used as shown in Table 2.

Mass Spectrometry Conditions The mass spectrometer was operated using the ESI source in positive ion mode. To optimize all of the MS parameters, standard solutions (100 ng/mL) and internal standard were infused into the mass spectrometer at a flow rate of 250 μL/min. The ion spray voltage (IS) was set at 4500 V. The TurboIonSpray probe temperature was maintained at 600°C. The instrument parameters *viz.*, nebulizer gas, curtain gas, auxiliary gas, and collision gas, were set at 60, 15, 80, and 5, respectively. Compound parameters *viz.*, declustering potential, collision energy, entrance potential, and collision exit potential, were 40, 20, 10, and 15, respectively, for 6β-hydroxytestosterone and [$^2H_7$]6β-hydroxytestosterone. Zero air was used as the source gas, while nitrogen was used as both curtain and collision gas. The mass spectrometer was operated in ESI positive ion mode and detection of the ions was performed in the multiple reaction monitoring (MRM) mode, monitoring the transition of *m/z* 305 precursor ion [M+H] to the *m/z* 269 product ion for 6β-hydroxytestosterone (retention time 8.7 min) and *m/z* 312 precursor ion [M+H] to the *m/z* 276 product ion for

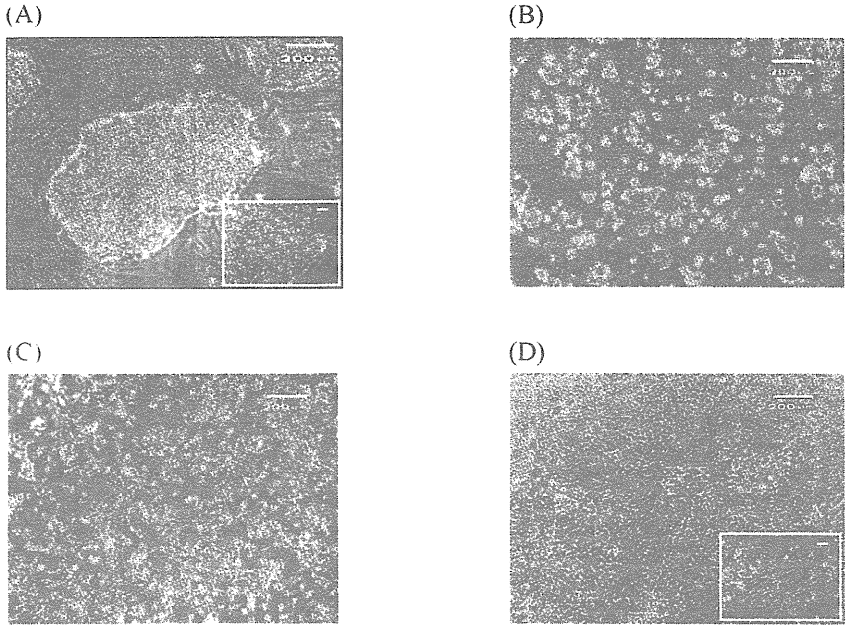

Fig. 2. Morphology of cmESCs in Individual Culture Processes

(A) Undifferentiated cmESCs. (B) Suspended cmESCs incubated on gelatin-coated plates for 2 h. (C) cmESCs cultured on plates 6 cm in diameter coated with Matrigel reduced (25-fold dilution) for 24 h. (D) cmESC-derived cells at 27 d after the initiation of hepatocyte differentiation. The cells were visualized by phase microscopy. Bars, 200 μm; 30 μm for A and D insets.

[^{2}H]6β-hydroxytestosterone (8.7 min). Quadrupoles Q1 and Q3 were set to unit resolution. Data acquisition and quantification were performed using Analyst software version 1.4.2 (Applied Biosystems, MDS Sciex, Toronto, ON, Canada).

Calibration Standards Calibration standards to cover the assay range of 10–5000 nM 6β-hydroxytestosterone were prepared by adding 10 μL of 0.1, 0.5, 1, 5, 10, and 50 μM working standards to 0.1 mL aliquots of control reaction mixture.

Statistical Analysis Statistical significance was assessed using the unpaired t test. In all analyses, $p < 0.05$ was taken to indicate statistical significance.

RESULTS

Morphology of cmESCs at Individual Culture Steps A typical colony of undifferentiated cmESCs is shown in Fig. 2A. As reported previously for primate ESCs, undifferentiated cmESCs formed tightly packed and flat colonies.[3] Each cell had a high nucleus cytoplasm ratio and prominent nucleolus. In an effort to circumvent the problem of apoptosis in cmESC culture, the single-cell dispersed culture was performed under feeder-free cell culture conditions using Y-27632. The undifferentiated cmESCs were cultured in the presence of 10 μM Y-27632 for 1 h before detaching the cells from the feeder layer. After the cmESC colonies were dissociated by trypsin and suspended, the cells were seeded on gelatin-coated plates. In this procedure, contaminating MEF adhered to the plate bottom, whereas the cmESCs did not (Fig. 2B). The cmESC clumps were recovered from the suspension and dissociated into single cells by pipetting. The single cells were cultured on culture plates 6 cm in diameter coated with Matrigel reduced (25-fold dilution) in the presence of 10 μM Y-27632 for first 24 h. The cmESCs proliferated on the feeder-free culture plates (Fig. 2C). Twenty-seven days after initiation of hepatocyte differentiation, cells showed characteristic morphologies of hepatocytes, *i.e.*, polygonal in shape and multiple nuclei (Fig. 2D). Y-27632 was effective for cmESC survival under dispersion culture conditions.

Expression of Hepatocyte Markers and CYP Enzymes in Primary cmHCs and cmESC-Derived Hepatocytes The mRNA expression levels of hepatocyte marker genes and CYP enzymes in primary cmHCs and differentiated cells from cmESCs were measured by a real-time PCR method. As shown in Fig. 3, the mRNAs of hepatocyte marker genes, α-fetoprotein (AFP), albumin (ALB), and CYP7A1, were detected in cmESC-derived hepatocytes together with those of CYP1A1, cmCYP2B6 (2B30), cmCYP2C9 (2C43), cmCYP2D6 (2D17), cmCYP3A4 (3A8), cmCYP3A5 (3A66), pregnane X receptor (PXR), and aryl hydrocarbon receptor (AhR). The mRNA levels of AFP and CYP7A1 in differentiated cells from cmESCs were 16- and 21-fold, respectively, higher than those in primary cmHCs, although the expression level of ALB was approximately 80-fold lower in cmESC-derived hepatocytes than in primary cmHCs. The mRNA levels of CYP1A1, cmCYP2B6 (2B30), cmCYP2C9 (2C43), cmCYP2D6 (2D17), cmCYP3A4 (3A8), cmCYP3A5 (3A66), and PXR in the cells differentiated from cmESCs were 386-, 7.4-, 284-, 1.6-, 136-, 5.9-, and 13-fold, respectively, lower than those in primary cmHCs. In contrast, the expression level of AhR mRNA in cmESC-derived hepatocytes was 2.2-fold higher than that in primary cmHCs.

Testosterone 6β-Hydroxylase Activity of Primary cmHCs and cmESC-Derived Hepatocytes Testosterone 6β-hydroxylase activity as a marker of CYP3A, especially cmCYP3A4 (3A8), was evaluated with primary cmHCs and cmESC-derived hepatocytes. Testosterone 6β-hydroxylase activity was detected in the cells differentiated from cmESCs (Fig. 4). The activity was about one sixth that of the primary

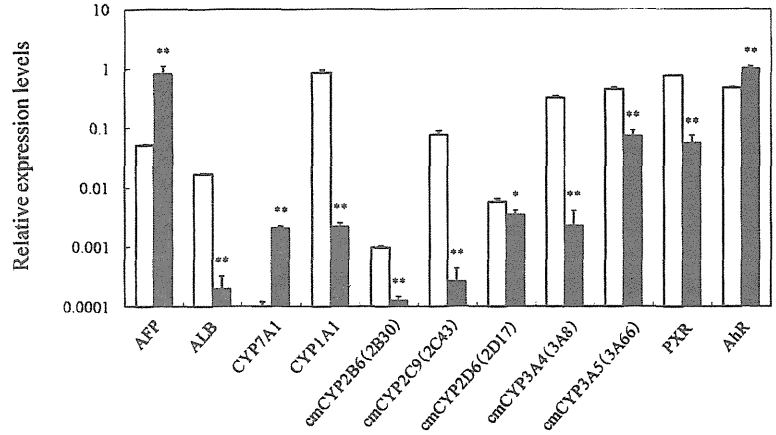

Fig. 3. Expression Levels of mRNAs for Hepatocyte Markers and CYP Enzymes in Primary cmHCs and cmESC-Derived Hepatocytes

Target mRNAs were analyzed by SYBR Green real-time PCR as described in Materials and Methods. Data are presented as the relative levels (means±S.D., n=3) of primary cmHCs (open columns) or cmESC-derived hepatocytes (closed columns) to adult monkey liver. Significantly different from primary cmHCs ($*p < 0.05$, $**p < 0.01$).

cmHCs.

Effects of RIF on the Expression Level and Activity of cmCYP3A4 (3A8) in the Cells Differentiated from cmESCs The induction potency of cmCYP3A4 (3A8) by RIF, which is known as a cmCYP3A4 (3A8) inducer,[13,14] was examined with the cells differentiated from cmESCs. The expression of cmCYP3A4 (3A8) mRNA was significantly induced by RIF in the cmESC-derived hepatocytes (Fig. 5A). The activity of testosterone 6β-hydroxylase in the cmESC-derived hepatocytes was significantly enhanced by RIF (Fig. 5B).

DISCUSSION

The method to induce differentiation of ESCs to hepatic cells was first established using mouse cells.[15–17] Many of these methods involve a procedure to differentiate ESCs by EB formation and adhesion culture. EBs differentiate into three embryonic germ layers by suspended cell culture of ESCs, and these cells can then further differentiate into multiple cell types, including hepatocytes, *in vitro*.[18] This method was applied to the induction of differentiation of monkey ESCs into hepatic cells.[7] In recent studies, however, a method to add some direct inducing factors to a monolayer culture system of an undifferentiated ESC colony without EB formation has been used extensively. Furthermore, some improved methods for more efficient differentiation into hepatocytes have been reported. Among these methods, the stepwise addition of two or more factors is most common.[19–23] However, if these complicated operations are not performed adequately, the death of ESCs can easily occur. In previous culture systems, remarkable reduction of the number of live cells was a technical obstacle to the induction of differentiation. Watanabe *et al.*[11] found that the death of human ESCs occurring after cell dissociation is triggered by activation of ROCK, and that the ROCK inhibitor Y-27632 can control the death of ESCs. Interestingly, Takehara *et al.*[12] demonstrated that Y-27632 also promotes survival of cmESCs and enables expansion from single cells without loss of their pluripotent characteristics. These findings suggest that reactions to the ROCK inhibitor may be preserved in primate ESCs. In addition, it has been shown that Y-27632 supplementation also enables cmESC

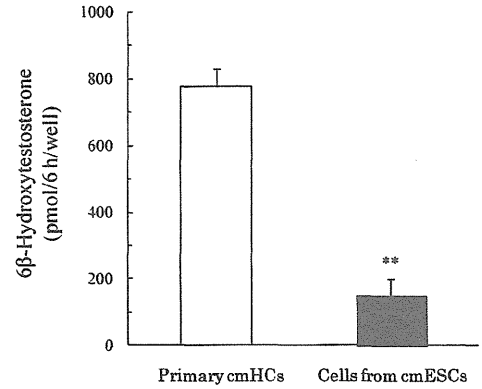

Fig. 4. Testosterone 6β-Hydroxylase Activity of Primary cmHCs and cmESC-Derived Hepatocytes

Primary cmHCs and cmESC-derived hepatocytes were incubated with testosterone at a final concentration of 100 μM for 6 h. Testosterone 6β-hydroxylase activity as a marker of CYP3A, especially cmCYP3A4 (3A8), was measured by LC-MS/MS as described in Materials and Methods. Values are expressed as the means±S.D. (n=3). Significantly different from primary cmHCs ($**p<0.01$).

expansion in feeder-free culture.[12] Feeder cells supply secretory components, extracellular matrix, and intercellular contacts for maintenance of an undifferentiated state and pluripotency of ESCs. However, the use of feeder cells leads to the potential for cross-contamination, such as the passing of animal pathogens to ESCs. On the other hand, feeder-free culture is a system to maintain ESCs in an undifferentiated state without direct contact with feeder cells. The ROCK inhibitor, Y-27632, is an important factor to enable adhesion and proliferation of primate ESCs in feeder-free culture. In the present study, we confirmed that dissociated cmESCs treated with Y-27632 were protected from cell death in feeder-free culture and formed clumps (Fig. 2B). Furthermore, the cells differentiated from cmESCs showed multinuclear morphology characteristic of hepatocytes at the final stage of differentiation (Fig. 2D). This feeder-free dispersion culture method was reproducible without any technical obstacles.

Although ALB is the most abundant protein synthesized by mature hepatocytes, its expression starts in early fetal hepatocytes and reaches the maximal level in adult hepatocytes.[24] Our study showed that the expression of ALB mRNA in

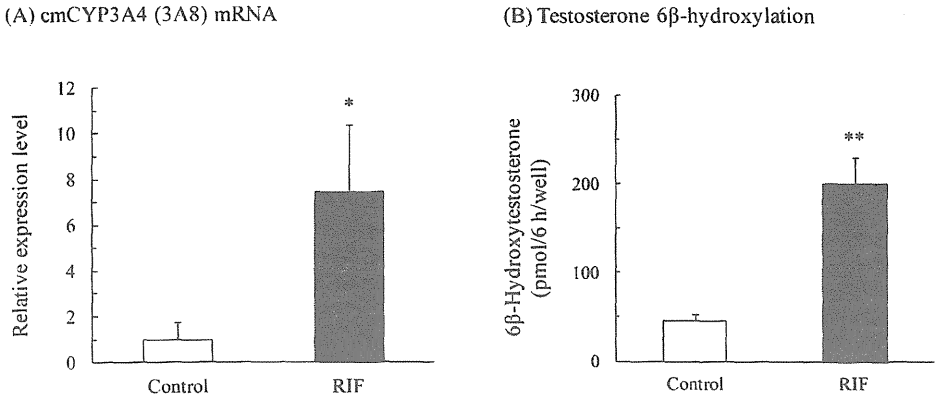

Fig. 5. Effects of RIF on cmCYP3A4 (3A8) mRNA Expression Level and Testosterone 6β-Hydroxylase Activity in Cells Differentiated from cmESCs

cmESC-Derived hepatocytes were treated with vehicle (0.1% DMSO) or 40 μM RIF for 72 h. After treatment with RIF, the cells were incubated with testosterone at a concentration of 100 μM for 6 h. (A) cmCYP3A4 (3A8) mRNA was analyzed by SYBR Green real-time PCR as described in Materials and Methods. Data are presented as the relative levels (means±S.D., n=3) of RIF treatment to vehicle treatment. (B) Testosterone 6β-hydroxylase activity was measured by LC-MS/MS as described in Materials and Methods. Significantly different from control (*p<0.05. **p<0.01).

hepatocytes differentiated from cmESCs was markedly lower than in primary cmHCs and adult monkey liver. On the other hand, AFP is a marker of endodermal differentiation as well as an early fetal hepatic marker; its expression level decreases as the liver develops into the adult phenotype. In this study, the expression of AFP mRNA in cmESC-derived hepatocytes was higher than that in primary cmHCs, although the mRNA level in the former cells was comparable to that in adult monkey liver. These results suggest that cmESC-derived hepatocytes may be differentiated into more immature cells rather than into mature cells.

CYP1A1 is a major CYP1A isoform expressed in the monkey liver,[25] in contrast to the human liver, which mainly expresses CYP1A2 but not CYP1A1.[26] cmCYP2B6 (2B30), cmCYP2C9 (2C43), cmCYP2D6 (2D17), cmCYP3A4 (3A8), and cmCYP3A5 (3A66) are major CYP enzymes in the cynomolgus monkey liver.[27] These monkey CYP enzymes show a high degree of amino acid sequence identity (>90%) with corresponding human CYP enzymes and catalyze typical drug oxidations of corresponding human CYP isoforms.[28] To characterize the expression of CYP1A1, cmCYP2B6 (2B30), cmCYP2C9 (2C43), cmCYP2D6 (2D17), cmCYP3A4 (3A8), and cmCYP3A5 (3A66) in hepatocytes differentiated from cmESCs, the basal gene expression patterns of these CYP enzymes were compared with primary cmHCs. The expression levels of the CYP enzymes examined were lower in cmESC-derived hepatocytes than in primary cmHCs. The lower expression of these CYP enzymes may be associated with hepatocyte maturity. In this study, the cmESC-derived hepatic cells were found to express cmCYP3A4 (3A8) mRNA. This enzyme function in differentiated hepatocytes was confirmed by testosterone 6β-hydroxylase activity. To our knowledge, this is the first study showing the functional expression of certain CYP enzyme in cmESC-derived hepatic cells. Furthermore, these cells showed inducibility of cmCYP3A4 (3A8) by RIF at mRNA and activity levels. This inducibility was qualitatively reproducible. The effects of RIF on mRNA expression of cmCYP3A4 (3A8) in the cmESC-derived hepatic cells was consistent with the findings reported previously.[7] It was previously reported that cmCYP3A4 (3A8) is induced by RIF through the transcription factor PXR.[29] Our study showed that PXR is expressed in cmESC-derived hepatic cells. These results suggest that PXR is active in these hepatocytes. This has important implications for the application of cmESC-derived hepatic cells as an *in vitro* model for drug development. However, the functional significance of cmCYP3A4 (3A8) and PXR in cmESC-derived hepatocytes was limited in this study because the data were partially qualitative. Further improvements are required, particularly with regard to maturation and quantitative analysis, for use of cmESC-derived hepatocytes in drug screening.

In conclusion, cmESCs were successfully differentiated into hepatocytes under feeder-free dispersion culture conditions supplemented with Y-27632. In addition, the basal expression and drug inducibility of CYP enzymes were characterized in these hepatocytes. These results suggest that cmESC-derived hepatocytes may be used as a potential source for stable supply of hepatocytes for drug metabolism analysis, although further investigations are needed to improve this method.

Acknowledgments This work was partly supported by Grants-in-Aid from the Ministry of Education, Culture, Sports, Science and Technology of Japan (Nos. 20926015, 22926013, and 23926012). We also thank Ms. K. Aikawa for technical assistance. We are grateful to Tanabe Seiyaku Co., Ltd. (Osaka, Japan) for generously providing cmESCs (CMK6).

REFERENCES

1) Thomson JA, Itskovitz-Eldor J, Shapiro SS, Waknitz MA, Swiergiel JJ, Marshall VS, Jones JM. Embryonic stem cell lines derived from human blastocysts. *Science*, **282**, 1145–1147 (1998).
2) Davila JC, Cezar GG, Thiede M, Strom S, Miki T, Trosko J. Use and application of stem cells in toxicology. *Toxicol. Sci.*, **79**, 214–223 (2004).
3) Reubinoff BE, Pera MF, Fong CY, Trounson A, Bongso A. Embryonic stem cell lines from human blastocysts: somatic differentiation *in vitro*. *Nat. Biotechnol.*, **18**, 399–404 (2000).
4) Suemori H, Tada T, Torii R, Hosoi Y, Kobayashi K, Imahie H, Kondo Y, Iritani A, Nakatsuji N. Establishment of embryonic stem

cell lines from cynomolgus monkey blastocysts produced by IVF or ICSI. *Dev. Dyn.*, **222**, 273–279 (2001).
5) Ginis I, Luo Y, Miura T, Thies S, Brandenberger R, Gerecht-Nir S, Amit M, Hoke A, Carpenter MK, Itskovitz-Eldor J, Rao MS. Differences between human and mouse embryonic stem cells. *Dev. Biol.*, **269**, 360–380 (2004).
6) Suemori H, Nakatsuji N. Generation and characterization of monkey embryonic stem cells. *Methods Mol. Biol.*, **329**, 81–89 (2006).
7) Momose Y, Matsunaga T, Murai K, Takezawa T, Ohmori S. Differentiation of monkey embryonic stem cells into hepatocytes and mRNA expression of cytochrome p450 enzymes responsible for drug metabolism: comparison of embryoid body formation conditions and matrices. *Biol. Pharm. Bull.*, **32**, 619–626 (2009).
8) Lavon N, Benvenisty N. Study of hepatocyte differentiation using embryonic stem cells. *J. Cell. Biochem.*, **96**, 1193–1202 (2005).
9) Asahina K, Fujimori H, Shimizu-Saito K, Kumashiro Y, Okamura K, Tanaka Y, Teramoto K, Arii S, Teraoka H. Expression of the liver-specific gene Cyp7a1 reveals hepatic differentiation in embryoid bodies derived from mouse embryonic stem cells. *Genes Cells*, **9**, 1297–1308 (2004).
10) Heo J, Factor VM, Uren T, Takahama Y, Lee JS, Major M, Feinstone SM, Thorgeirsson SS. Hepatic precursors derived from murine embryonic stem cells contribute to regeneration of injured liver. *Hepatology*, **44**, 1478–1486 (2006).
11) Watanabe K, Ueno M, Kamiya D, Nishiyama A, Matsumura M, Wataya T, Takahashi JB, Nishikawa S, Nishikawa S, Muguruma K, Sasai Y. A ROCK inhibitor permits survival of dissociated human embryonic stem cells. *Nat. Biotechnol.*, **25**, 681–686 (2007).
12) Takehara T, Teramura T, Onodera Y, Kakegawa R, Fukunaga N, Takenoshita M, Sagawa N, Fukuda K, Hosoi Y. Rho-associated kinase inhibitor Y-27632 promotes survival of cynomolgus monkey embryonic stem cells. *Mol. Hum. Reprod.*, **14**, 627–634 (2008).
13) Nishimura M, Koeda A, Suganuma Y, Suzuki E, Shimizu T, Nakayama M, Satoh T, Narimatsu S, Naito S. Comparison of inducibility of CYP1A and CYP3A mRNAs by prototypical inducers in primary cultures of human, cynomolgus monkey, and rat hepatocytes. *Drug Metab. Pharmacokinet.*, **22**, 178–186 (2007).
14) Ohtsuka T, Yoshikawa T, Kozakai K, Tsuneto Y, Uno Y, Utoh M, Yamazaki H, Kume T. Alprazolam as an *in vivo* probe for studying induction of CYP3A in cynomolgus monkeys. *Drug Metab. Dispos.*, **38**, 1806–1813 (2010).
15) Hamazaki T, Iiboshi Y, Oka M, Papst PJ, Meacham AM, Zon LI, Terada N. Hepatic maturation in differentiating embryonic stem cells *in vitro*. *FEBS Lett.*, **497**, 15–19 (2001).
16) Chinzei R, Tanaka Y, Shimizu-Saito K, Hara Y, Kakinuma S, Watanabe M, Teramoto K, Arii S, Takase K, Sato C, Terada N, Teraoka H. Embryoid-body cells derived from a mouse embryonic stem cell line show differentiation into functional hepatocytes. *Hepatology*, **36**, 22–29 (2002).
17) Maezawa K, Miyazato K, Matsunaga T, Momose Y, Imamura T, Johkura K, Sasaki K, Ohmori S. Expression of cytochrome P450 and transcription factors during *in vitro* differentiation of mouse embryonic stem cells into hepatocytes. *Drug Metab. Pharmacokinet.*, **23**, 188–195 (2008).
18) Doetschman TC, Eistetter H, Katz M, Schmidt W, Kemler R. The *in vitro* development of blastocyst-derived embryonic stem cell lines: formation of visceral yolk sac, blood islands and myocardium. *J. Embryol. Exp. Morphol.*, **87**, 27–45 (1985).
19) Cai J, Zhao Y, Liu Y, Ye F, Song Z, Qin H, Meng S, Chen Y, Zhou R, Song X, Guo Y, Ding M, Deng H. Directed differentiation of human embryonic stem cells into functional hepatic cells. *Hepatology*, **45**, 1229–1239 (2007).
20) Agarwal S, Holton KL, Lanza R. Efficient differentiation of functional hepatocytes from human embryonic stem cells. *Stem Cells*, **26**, 1117–1127 (2008).
21) Hay DC, Zhao D, Fletcher J, Hewitt ZA, McLean D, Urruticoechea-Uriguen A, Black JR, Elcombe C, Ross JA, Wolf R, Cui W. Efficient differentiation of hepatocytes from human embryonic stem cells exhibiting markers recapitulating liver development *in vivo*. *Stem Cells*, **26**, 894–902 (2008).
22) Touboul T, Hannan NR, Corbineau S, Martinez A, Martinet C, Branchereau S, Mainot S, Strick-Marchand H, Pedersen R, Di Santo J, Weber A, Vallier L. Generation of functional hepatocytes from human embryonic stem cells under chemically defined conditions that recapitulate liver development. *Hepatology*, **51**, 1754–1765 (2010).
23) Zhou M, Li P, Tan L, Qu S, Ying QL, Song H. Differentiation of mouse embryonic stem cells into hepatocytes induced by a combination of cytokines and sodium butyrate. *J. Cell. Biochem.*, **109**, 606–614 (2010).
24) Sellem CH, Frain M, Erdos T, Sala-Trepat JM. Differential expression of albumin and alpha-fetoprotein genes in fetal tissues of mouse and rat. *Dev. Biol.*, **102**, 51–60 (1984).
25) Sakuma T, Hieda M, Igarashi T, Ohgiya S, Nagata R, Nemoto N, Kamataki T. Molecular cloning and functional analysis of cynomolgus monkey CYP1A2. *Biochem. Pharmacol.*, **56**, 131–139 (1998).
26) Schweikl H, Taylor JA, Kitareewan S, Linko P, Nagorney D, Goldstein JA. Expression of CYP1A1 and CYP1A2 genes in human liver. *Pharmacogenetics*, **3**, 239–249 (1993).
27) Uehara S, Murayama N, Nakanishi Y, Zeldin DC, Yamazaki H, Uno Y. Immunochemical detection of cytochrome P450 enzymes in liver microsomes of 27 cynomolgus monkeys. *J. Pharmacol. Exp. Ther.*, **339**, 654–661 (2011).
28) Iwasaki K, Uno Y. Cynomolgus monkey CYPs: a comparison with human CYPs. *Xenobiotica*, **39**, 578–581 (2009).
29) Kim S, Dinchuk JE, Anthony MN, Orcutt T, Zoeckler ME, Sauer MB, Mosure KW, Vuppugalla R, Grace JE Jr, Simmermacher J, Dulac HA, Pizzano J, Sinz M. Evaluation of cynomolgus monkey pregnane X receptor, primary hepatocyte, and *in vivo* pharmacokinetic changes in predicting human CYP3A4 induction. *Drug Metab. Dispos.*, **38**, 16–24 (2010).